

Sedimentary blue carbon dynamics based on chrono-sequential observation in a tropical restored mangrove forest

Raghab Ray^{1*}, Rempei Suwa², Toshihiro Miyajima¹, Jeffrey Munar³, Masaya Yoshikai⁴, Maria Lourdes San Diego-McGlone³, Kazuo Nadaoka⁴

5 ¹*Atmosphere and Ocean Research Institute, The University of Tokyo, Kashiwa
raghab.ray@aori.u-tokyo.ac.jp; miyajima@aori.u-tokyo.ac.jp*

² *Japan International Research Center for Agricultural Sciences, Tsukuba
swrmp2005@yahoo.co.jp*

³ *Marine Science Institute, University of the Philippines, Diliman
mlmcglone@msi.upd.edu.ph; jcmunar1@up.edu.ph*

10 ⁴ *School of Environment and Society, Tokyo Institute of Technology, Tokyo
yoshikai.m.aa@m.titech.ac.jp; nadaoka.k.aa@m.titech.ac.jp*

Correspondence to: Raghab Ray (raghab.ray@aori.u-tokyo.ac.jp, raghab.ray@gmail.com)

15

Abstract. Among many ecosystem services provide by mangroves, macro-climate regulation via the storage of large amounts of organic carbon (OC) in marine sediments (also known as ‘blue carbon’) has given these unique ecological environments mangroves enormous global attention, due to their role in climate change mitigation. While there are many studies on blue carbon potential of intact mangroves (i.e. naturally growing), there have been very few studies 20 on restored mangroves (i.e. planted). This study aims to address this knowledge gap by examining the sediment development process during early colonization (rehabilitation) of mangroves in an OC-poor estuary in the Panay Island, Philippines. Based on endmember-source apportionment of multiple endmembers in the sedimentary organic matter, the contribution of mangrove plant material was higher at the older sites compared to the younger sitesettings 25 or bare sediments where there is more contribution of riverine input. A clear increasing gradient according to mangrove development was observed for bulk OC (0.06 to 3.4 $\mu\text{mol g}^{-1}$), porewater OC (292 to 2150 $\mu\text{mol L}^{-1}$), sedimentary OC stocks (3.13 to 77.4 Mg C ha^{-1}) and OC loading per surface area (7 to 223 $\mu\text{mol m}^{-2}$). The estimate of carbon accumulation rates (6 to 33 $\text{mol m}^{-2} \text{yr}^{-1}$) based on chrono-sequence are within the global ranges and show an increasing pattern with the age of mangrove sage. Hence, the sediment of relatively young mangrove forests appear to be significant potential C sink, and short term chrono-sequence based observationsmethod can efficiently define the importance of mangrove restoration programs as a potential carbon sequestration pathway. Although a differential yet systematic pattern of increasing OC sink based on short-term chrono-sequence can define the role of a mangrove rehabilitation program, there is a need for long term monitoring to verify the consistently elevated OC with mangrove growth.

1. Introduction

- Formatted: Font: (Default) Times New Roman, 10 pt
- Formatted: Font: (Default) Times New Roman, 10 pt
- Formatted: Font: (Default) Times New Roman, 10 pt
- Formatted: Font: (Default) Times New Roman, 10 pt
- Formatted: Font: (Default) Times New Roman, 10 pt
- Formatted: Font: (Default) Times New Roman, 10 pt
- Formatted: Font: (Default) Times New Roman, 10 pt
- Formatted: Font: 10 pt

35 The term 'Blue Carbon' was first introduced more than a decade ago to describe the large quantity of organic carbon (OC) present in shallow coastal habitats like mangroves (Nellemann et al., 2009). Mangroves, located around the tropical and subtropical coastal regions are known for storing significant amounts of OC in the sediment and vegetation biomass. Out of the typical total carbon stocks of 739 ± 28 Mg C ha^{-1} in mangrove ecosystems, sediment OC accounts for 73–79 % (down to 1 m depth) while above- (AGB) and below-ground root biomass (BGB) account for 14–15% and 8–9%, respectively (Alongi, 2020; Hatje et al., 2020; Walcker et al., 2018). Mangrove sediment is the largest depository of OC owing to their efficiency in trapping suspended sediments and associated sedimentary organic matter (SOM), high algal OM (benthic algae and phytoplankton) and vascular plant-derived OM and low decomposition rates of SOM under anoxic conditions in the sediment. A $\sim 0.5m$ to 3m depth core generally represent ~ 49 to 98% of ecosystem OC stocks, (Donato et al., 2011) and sediment depth in the undisturbed mangrove forest sites can often exceed to 3 m (Elwin et al., 2019). The high C sink capacity of mangroves makes them one of the key ecosystems that contribute to climate change mitigation by capturing large amounts of atmospheric CO₂ (Howard et al., 2017). However, there has been a rapid loss of mangroves due to land use and deforestation that has resulted the release of OC stored in the sediments back to the atmosphere as CO₂ (Valiela et al., 2001). For instance, conversion of mangroves to aquaculture ponds, paddy fields, and pastures, and removal of mangrove tree removal have resulted in OC stocks per unit area becoming $1/8^{th}$ to $1/2^{th}$ 2 to 8 times lower than of the intact mangrove forests (Salmo et al., 2013; Kauffman et al., 2017; Sharma et al., 2020). Therefore, the quantification of blue C stock and sequestration rate provides added value for mangrove protection to ecosystem services and serves as a useful management tool when implementing plans for mangrove sustainability and productivity (Sheehan et al., 2019). During the last three decades, several countries have implemented mangrove rehabilitation and restoration programs effectively to reverse mangrove forest cover loss. However, Mangrove restoration efforts such as Reducing Emissions from Deforestation and forest Degradation (REDD+) have considered C emission loss only from above-ground biomass -reduced C emissions by considering loss from the above ground biomass part only (Pendleton et al., 2012). Countries like the Philippines have started to address REDD+, loss of mangroves, and degradation of blue C habitats through their policies and rehabilitation management plans. To assess the effectiveness of such efforts, there should be a comparison between the intact and restored mangrove forests in terms of sediment OC stocks and accumulation rates. Restored mangrove forests are rarely explored globally with some notable exceptions in the subtropical coastal regions of China (Ren et al., 2010; Lunstrum and Chen, 2014; Wang et al., 2021), and Vietnam (Van Hieu et al., 2017; Dung et al., 2016). Chrono-sequence is an indirect approach or a type of 'natural experiment' (Pickett, 1989) that can be applied to the relatively younger sites (e.g., Bakhawan Ecopark, Philippines, examined in this study) where all environmental and biological conditions of the experimental sites must be identical except for the age, and species diversity is low (Nilsson and Wilson, 1991; Walker et al., 2010). In this study, an evaluation based on chrono-sequential observation (a.k.a. "space for time substitution" or SFT; Pickett, 1989) is made for sites in the Philippines where restoration is a viable option. In this study, an evaluation based on a type of 'natural experiment' or chrono-sequence (a.k.a. "space-for-time-substitution" or SFT; Pickett, 1989) is conducted at a relatively younger site (e.g., mangrove ecopark, Philippines, examined in this study) wherein to fulfill conditions for chrono-sequence, all environmental and

Formatted: Space After: 8 pt, Line spacing: 1.5 lines

Formatted: Font: (Default) Times New Roman, 10 pt

Formatted: Superscript

Formatted: Superscript

Formatted: Font: 10 pt

Formatted: Font: 10 pt

Formatted: Font: 10 pt

Formatted: Font: 10 pt

biological conditions of the experimental sites must be identical except for the age, and species diversity is low
(Nilsson and Wilson, 1991; Walker et al., 2010).

75 The judicious use of chrono-sequential observation or SFT has already advanced our understanding of short-term temporal dynamics of carbon in naturally expanding mangroves (e.g., 66-year extent in^{by} Walcker et al., 2017⁷⁸; 70-year extent in^{by} Kelleway et al., 2016).

78 The capacity of nearshore vegetated habitats as blue carbon sink is controlled by geophysical constraints such as sediment supply rate, depositional conditions, and tidal elevation (Miyajima et al., 2017; Jiménez-Arias et al., 2020). Based on chrono-sequential studies of the naturally occurring mangroves intact mangroves, OC accumulation in sediments increased with tree age, and OC sources change spatially with mangrove development (Lovelock et al., 80 2010; Marchand et al., 2017; Walcker et al., 2018). Most of the OC stored in mangrove sediments change at the spatial scale from plant-derived OM at the interior mangrove sites to algal OM at the proximal tidal flat (Gontharet et al., 2014; Prasad et al., 2017; Ray et al., 2018). With the development of mangroves, higher vascular plant or mangrove-derived OC sources may dominate the OM pool (Marchand et al., 2006). A significant fraction of mangrove-derived OC that has accumulated on top of the bare sediment can be washed away to the nearshore waters by tidal action 85 (Brown et al., 2021; Ray et al., 2020). By considering bare sediments and old growth mangrove stands as two extreme ends of a transect that consists of mangroves with different ages, a systematic overview of sedimentary blue C dynamics can be captured for restored mangroves. The Stable isotope ratio of carbon ($\delta^{13}\text{C}$) is frequently used to evaluate the relative contributions of end member sources to the OM pool through mixing models with either $\delta^{15}\text{N}$ or C:N ratios (Ray and Shahraki 2016; Sasmito et al., 2020). The use of such biogeochemical controls on blue C dynamics 90 has rarely been reported for the restored mangroves (e.g., Kandelia dominated forest reported by, Van Hiew et al., 2017).

95 In this study, we address the question of how chrono-sequential observation in a restored mangrove forest could guide us in achieving an improved scientific understanding of C sources, stocks, and monitor the changes in accumulation rates in the early development stage and adult stages. Where, we hypothesize that the restored mangroves increase sediment C storage in accordance with maturity of vegetation. To test this, we (1) calculated the total OC (TOC), dissolved OC (DOC), and OC accumulation rate along a chrono-sequence of restored mangroves forests located in the Philippines, and (2) examined how blue C varies with sedimentary geochemical properties (OC, bulk density, specific surface area). The Isotopic signatures such as $\delta^{13}\text{C}$ which allows for an efficient provenance analysis of SOM 100 wereas also examined. Additionally, particulate OC (POC) present in the surface water was analyzedexamined to assign different end member sources in the SOM pool (e.g., plant organ, riverine and pelagic algae).

2. Material and Methods

2.1. Study area

105 Sampling was conducted in a planted mangrove forest, locally known as Bakhawan Ecopark, located in Kalibo eCity inon Panay Island in Central Philippines during the wet season (September 2018 and 2019) and dry season (February 2019) (Fig. 1, $11^{\circ} 43' 42''\text{-N}$, $122^{\circ} 23' 39.12''\text{-E}$). The Bakhawan Ecopark is the remnant area of a former deltaic

Formatted: Font: 10 pt, Font color: Text 1, English (United Kingdom)

mangrove at the mouth of the Aklan River (Duncan et al., 2016). Aklan River which has a drainage area of 852 km² flows into the northwestern coastal area of Kalibo, continuously depositing high sediment yield to form the alluvial plain down the river. Sediments entrained by the longshore current formed sandbars, beach ridges, and coalesced mouthbar deposits. To prevent the damages by coastal flooding, a large portion of the sea facing mudflat were planted 110 with 45 ha of *Rhizophora apiculata* and 5 ha of *Nypa fruticans* in 1990 by a cooperative comprised of local families (Kalibo Save the Mangrove Association or KASAMA). An additional 20 ha of *Rhizophora* spp. were planted in 1993 (Primavera, 2004) for the purpose of stabilizing the shoreline, decreasing sedimentation to the offshore, and increasing 115 fish stocks and wood production (Department of Environment and Natural Resources or DENR, Philippines). Insect damage of the plantation in 1997 was followed by infilling of naturally-recruited *Avicennia marina* and *Sonneratia alba*. The seafront area was replanted in 2006 with *Rhizophora apiculata*, and subsequently recolonized naturally by 120 *A. marina* and *Sonneratia alba* (Duncan et al., 2016). New recruitment of both *A. marina* and *R. apiculata* took place on the mud bank in May/June 2019. The inland part of the Ecopark is dominated by naturally growing mangroves. Natural growth of mangrove trees and planting efforts since the 1990's at the Aklan River mouth stabilized and 125 enlarged the mangrove forest by at least 627%, to a flourishing 121 ha today. Based on remotely-sensed data, the land area of the forest has increased by 52.42% on average every five years since 1985. The Food and Agriculture Organization of the United Nations has cited the Bakhawan mangroves for excellence in forest management (Cadaweng & Aguirre 2005).

125 The Tide in the Bakhawan Ecopark is semidiurnal microtidal with the highest amplitude of around 2m. The mangrove forest floor is fully inundated during the high tide. At the mouth of the Aklan River, water meanders along a small channel between the sandbar and mangrove-lined coast. The climate of Aklan is categorized as Type III (according to the Philippines Atmospheric, Geo-Physical, and Astronomical Services Administration) with no pronounced maximum rain period except for short dry periods of 1–3 months (December to February or March to May). The rest of the year represents wet season with total annual rainfall of 3200±775 mm and mean temperature of 27.2 °C (2017-2018, JRA-55 reanalysis).

130 Sediment sampling locations were categorized according to mangrove ageing as bare sediment (BS, 0-yr), pioneer mangroves (PM, 0.25-yr), young mangrove (YM, 10-yr), adult mangrove (AM, 20-yr) and mature mangroves (MM, 30-yr). These categories are partly influenced by Marchand et al. (2003) who examined the chrono-sequential sedimentary OC in naturally growing *Avicennia* dominated mangroves in the French Guiana muddy coast. The center of the mangrove forest is dominated by AM and the sea facing edge of the Ecopark has decreasing mangrove 135 age from MM to PM. Both BS and PM are inundated during the high tide. *Rhizophora apiculata* is the dominant species at YM, AM and MM, while mixed mangroves (*Avicennia* and *Rhizophora* sp.) are found at PM. Among the two sites of bare sediments, BS1 which is closer to YM, was sampled during the wet season, while BS2 which is isolated from the mangrove sites, was sampled in the dry season, (Fig. 1). Mean tree heights were <1 m, 3–4 m, 6–8 m, 10–15 m for PM, YM, AM, and MM, respectively (data not shown).

140

2.2. Sampling procedure

145 Sediment thickness was measured at each site using a tool for cone penetration test (KS-159, Kansaiiiki Inc.)[•] (Yoshikai et al., 2021). Single cores ~~were~~ was collected at each site during ~~the~~ low tide by manually pushing a Eijkelkamp peat sampler (DIK-105A, ~~Ø~~-52mm ~~Ø~~, ~~length~~-50cm ~~length~~) into the sediment. A total of 8 cores were retrieved during the survey period with seasonal collection made ~~at~~from BS, AM, YM and MM ~~site (dry and wet seasons, a total of 6 cores) and from PM and YM sites (wet season, one core each)~~ sites. The GPS coordinates ~~of at~~ all sampling sites were recorded (Garmin MAP64s) to locate them again for duplicate sampling in a different season, (Garmin MAP64s). Immediately after sampling, each core was sectioned into 2-cm interval up to the first 10-cm and 5-cm interval beyond 10 cm depth. Average ~~The total~~ sample depth at BS, AM and MM were always 50 cm, while for PM and YM were 20 cm and 25 cm, respectively, each site was consistently around 50 cm. *In situ* pH (NBS scale), temperature and oxidation reduction potential (ORP, ~~AgCl-Pt~~-electrode) were recorded for each section using hand-held multiparameter probes (HORIBA pH-conductivity sensors, WTW redox sensor). About 0.8 to 1 kg cores were collected from each site. Visible root material, decaying plant matter and dead wood were removed from the sediment sample in the field. Samples were kept in styrofoam box and brought to the laboratory. Within 3-4 hours after collection, sediment samples were kept in styrofoam box and brought to the laboratory for analysis of bulk density, specific surface area (SSA), concentrations and isotope ratios of carbon and nitrogen, and carbon stock.

150

155

Formatted: Line spacing: 1.5 lines

160 Additional sediment cores for porewater sampling were collected by inserting PVC corer manually at each site (6.5cm inner diameter, 70 cm length). A total of 7 cores were retrieved on ~~a~~ seasonal basis (single core from each site per season). Immediately after retrieval, the top and bottom ends of the corer were closed using rubber caps. Rhizon tubes (Rhizosphere Research Products) were inserted to the holes drilled at specified intervals (0.5cm interval ~~untill~~ the first 4cm followed by 2 cm interval up to the 10_{cm}, and finally 5 cm interval). A Rhizon tube is a small microporous polymer tube (2.5 mm diameter, < 0.2 μ m pore size of the membrane) connected to a plastic syringe (25 ml capacity) by a standard luer-lock connector. Around 8–10 ml of porewater were extracted in ~~about an~~ 1 hour. Salinity of the extracted porewater was measured using a refractometer. Porewater was transferred to pre-combusted amber vials (20 mL) for dissolved organic carbon (DOC) analyses.

165

170 Tidal water sampling was conducted along the salinity gradient (0 to 33) in the Aklan River. For this study, three representative sites were chosen, the upstream of the Aklan River and outer-shore as potential endmember sources of SOM, and the river channel very close to BS site during ~~the~~ high tide. More details of water sampling techniques can be found in the supplementary material. A global tide prediction model (NAO.99b, Matsumoto et al., 2000) was used to correct water depth data to ~~the~~ relative elevation at each site from Mean Sea Level or MSL.

175 In the laboratory, pre-weighed wet sediment subsamples were oven dried at 60°C for 48 ~~hours~~ to allow for calculation of dry bulk density (BD) and water content. For sediment subsampling, open mouth plastic syringe was used (2 cm ~~inner diameter~~ and 1.5cm length). Bulk density (g cm^{-3}) was determined as the dry sediment weight (g) divided by the initial volume (cm^3). The ~~R~~est of the wet sediment samples were freeze dried using a Benchtop Freeze Dry System (Labconco). The freeze-dried samples were gently crushed using a mortar and pestle and passed through a 1 mm mesh

stainless steel sieve to remove the large gravel (referred to as the coarse fraction). The sieved samples were stored in tightly capped glass vials under <40% relative humidity.

2.3 Chemical analyses

180 The dried and homogenized sediment samples were subjected to acid treatment to remove inorganic carbon. Approximately 1 g of dried sample was placed into screw-capped glass tubes (10 mL), and 2.0 N hydrochloric acid (HCl) solution was added to the sediment dropwise until all the carbonate was converted to CO₂. After centrifugation for 15 min at 2000 rpm, followed by washing with deionized water and decantation, the final residue in the tube was dried at 60 °C overnight. Once cooled, the dried samples were weighed into a tin capsule (10 x 10 mm), folded and 185 kept temporarily in a 48-well microtiter plate until analysis.

The concentrations and isotope ratios of OC and total nitrogen (TN) in the treated samples were determined simultaneously by EA-IRMS (FLASH 2000/Conflo IV/DELTA V Advantage, ThermoFisher Scientific, Bremen, Germany). Two standard materials of different $\delta^{13}\text{C}$ (-26.4 to -19.6‰) and $\delta^{15}\text{N}$ (2.5 to 5‰) values (SI Science Ltd., Saitama, Japan) were used for calibration. The measured isotope ratios were represented using the conventional δ -notation ($\delta^{13}\text{C}$ and $\delta^{15}\text{N}$, in ‰) with Vienna Pee-Dee Belemnite and atmospheric N_2 as the reference materials. The instrumental analytical precision was normally within $\pm 1\%$ for the OC and TN concentrations and $\pm 0.1\%$ for $\delta^{13}\text{C}$ and $\delta^{15}\text{N}$.

195 Measurement of specific surface area (SSA) ~~in~~^{of the} sediment was performed by the multipoint Brunauer–Emmett–Teller (BET) method based on N₂ gas adsorption under reduced pressure (~~for~~ details refers to Miyajima et al., 2017).
196 Specific surface area was measured only for BS, AM and MM cores. The dried and homogenized sediment samples
197 were heated at 350 °C for 12 h followed by calculation of weight loss on heating after 1 hour. Between 0.5 g and 2.0
198 g of the treated samples were weighed into glass flasks and desiccated in vacuo at 350 °C for 3 h. Immediately after
199 cooling, a multipoint BET measurement was performed with N₂ (purity > 99.99%) as the adsorbate using a^{the}
200 BELSORP mini II (MicrotracBEL, Osaka, Japan) surface area analyzer. The slope of the BET plot in the linear region
201 was used for estimating the SSA.

2.4 Data analyses

The results of the OC and TN concentrations, and the SSA were expressed as μmol and m^2 per unit dry weight of bulk sediment, respectively. Carbon stocks (Mg C ha^{-1} , top 50 cm, referred to as S) of each core at the 5 sites were calculated on a seasonal basis as

Where C_n is the C concentration (mass %) and ρ_n is the bulk density (g cm^{-3}) of the sample, and l (cm) is the length of the sample section (i.e. depth zero to n^h). The amount of OC preserved per unit surface area of sediment particles is referred to as OC loading (OC/SSA in $\mu\text{mol m}^{-2}$; Mayer 1994).

Formatted: Superscript

In a chrono sequence study, it is common to apply linear regression model between mangrove age and C stock **s** and derive the slope, i.e., carbon accumulation rate (CAR) (Alongi, 2004; Walcker et al., 2018) or individually following the formula such as $CAR = [(C \text{ stock of the stand}) - (C \text{ stock of the previous stand})] / [(age \text{ of the stand}) - (age \text{ of the previous stand})]$ (Marchand et al., 2017). However, our results showed best-fit with the exponential function for the relationship.

where a and b are the constants determined from the field data best-fit exponential relationship as 100.34 and 0.058, respectively, and yr is the age of mangrove stands (years). Here we assume that with the exponential increase of plant above-ground mass with early mangrove growth, below-ground root mass also increases, which that contributes significantly to OC accumulation with early mangrove development. However, because the exact maturity stage of these mangroves is unknown, the typical logistic curve equation that is otherwise used for the matured forests, was not applied, instead the best-fitted exponential trend was used. Based on the exponential model, slope was derived for the individual sample following the equation:

Accordingly, CAR for the age class of mangroves (0.25, 5, 10, 15, 20, 25 and 30 year) was calculated and fitted with an exponential function following a non-linear least square method using *nls* function of the statistical software R ver. 4.0.2 (R development core team, 2020). The 95% confidence interval for the fitted model was computed with *predFit* function of *investr* package. The exponential model was compared with a simple linear regression model.

Accordingly, CAR for the age class of mangroves (0.25, 5, 10, 15, 20, 25 and 30 year) was calculated and fitted in the exponential curve and compared with the slope derived from the linear regression model.

To evaluate the effects of sampling Depth, Season and stand Types (i.e., chronology based) on $\delta^{13}\text{C}$, $\delta^{15}\text{N}$ and C:N ratio of SOM, the general additive linear mixed model (GAM) was constructed with a *gam* function in a R package (mgcv). Depth, Season, Types ([or sites based on chronology](#)), and an interaction between Season and Types were treated as fixed effects where Depth was incorporated into the model. Using the results of *gam*, ANOVA was used to evaluate the significance of each variable with a significance level at $p = 0.05$.

For subsequent provenance analysis, a binary source mixing model was applied (Parnell and Inger, 2016) based on the mean values of $\delta^{13}\text{C}$, $\delta^{15}\text{N}$ and C:N ratio of sediment samples from different depth in each core. The samples obtained in different seasons were treated as independent samples. In total, seven mean values were used for the analysis of Bayesian mix model using multiple R packages (RGtk2, MixSIAR, splanc). The endmember sources of OM chosen for this study were the green leaf of *Rhizophora apiculata*, POM (particulate organic matter) of marine and river water, and microphytobenthos (MPB). Among these endmembers except for POM, the $\delta^{13}\text{C}$, $\delta^{15}\text{N}$ and OC:TN ratio for green leaf and MPB were obtained from the literature (refers to Table S1). Although OC:TN values were shown to be largely variable between green (~30) and yellow/senescent leaves on the sediment floor (~50) of the *Rhizophora apiculata*, their $\delta^{13}\text{C}$ values were the same (~-28.5‰) (Nordhaus et al., 2017). For this similar reason,

the mangrove root is also not considered, instead leaf singularly representeds the-as mangrove-derived OC source. Hence it is reasonable for this study to choose green leaves and avoid redundant increase of endmembers for the model. Microphytobenthos located on the tidal flat between the interface of sea and land can also be variable depending on the $\delta^{13}\text{C}$ of dissolved inorganic carbon (photosynthesis substrate for MPB). This is similar to the riverine settings in French Guiana ('mixed MPB' -20.9‰, Ray et al., 2018), inand contrast to the oceanic setting in the Red Sea ('pure MPB' -17.9‰, Shahraki et al., 2014). The Nnumber of endmembers were chosen carefully keeping small standard deviation of $\delta^{13}\text{C}$ and OC:TN within each endmember and clearly separated with significant differences from each other (ANOVA, $p<0.05$). We refrained from considering a large number of endmembers, and omitted less important endmembers or treated collectively some endmembers whose isotopic and elemental compositions are similar (e.g., plant parts such as leaf, root, litter). Since there was no seagrass recorded at or around the sites, its potential endmember contribution to the mangrove SOM was ignored. On the contrary, although the isotopic composition of MPB and marine POM were not very different, we selected MPB as endmember due to its visible presence on the exposed tidal flat (BS2) during the low tide.

3. Results

Mangrove development with age is shown in Fig. 2a. Maximum elevation of 0.45 m from the MSL was measured at the mature mangrove (MM) site, and a minimum value of -1.3 m was recorded for the bare sediment (BS) (Fig. 2b). Mean porewater salinity, sediment temperature and pH did not vary significantly between the various stages of mangrove development (Figs. 2c-e). Sediment thickness was higher in mangrove sediment (140-265cm) than the tidal flat (<100 cm) (Fig. 2g). Sediment bulk density at the top 50 cm increased with decreasing mangrove age tending to be maximum at BS (0.6 to 1.3 g/cm³, Fig. 2j), n=93, Table 1. Specific surface area of the sediments varied from 9.8 to 21.2 g/m² g⁻¹ (Fig. 2j, n = 19) with the lowest value for the coarser bare sediment. The Ffraction of coarse sandlarge gravels (>1 mm mesh size) tend to be higher going seaward. A consistent increment in sediment OC concentration, (top 50 cm, n = 93), TOC:TN molar ratio (from YM to MM, n = 92), and porewater DOC (n = 64) was observed with the mangrove development (Figs. 2k-m), evolution (BS: 0.06 $\mu\text{mol/g}$, 21.9 mol/mol, and 292 $\mu\text{mol L}^{-1}$; at MM: 3.4 $\mu\text{mol g}^{-1}$, 19.7 mol/mol, and 2150 $\mu\text{mol L}^{-1}$, respectively). The mean value of bulk $\delta^{13}\text{C}$ became more negative (Fig. 2n), and the mean $\delta^{15}\text{N}$ became more positive with mangrove age ($\delta^{15}\text{N} = -1.15$ at the BS to 1.06 ‰ at AM, figure not shown), ($\delta^{13}\text{C} = -25.07$ ‰ at BS and -28.9‰ at MM, n = 93). The mean $\delta^{15}\text{N}$ varied from -1.15 at the BS to 1.06 ‰ at the adult mangrove (AM) site (n = 90). Organic carbon (OC) stock was determined to be maximum at the mature stand (93.577.4 Mg C/ha) and lowest at the bare sediment (3.13 Mg C/ha) (Fig. 2o). Similar to the trend of OC stock, OC loading varied widely between 4 and 380 $\mu\text{mol/m}^2$ (n = 19) (Fig. 2p), with mangrove sites having higher OC loading (mean: 152 $\mu\text{mol/m}^2$) than the bare sediment (25 $\mu\text{mol/m}^2$).

Vertical profile of sediment OC and $\delta^{13}\text{C}$, specific surface area (SSA) and OC loading, and porewater DOC on a seasonal basis are shown in Figs. 3–5. Sediment surface values (0-10 cm) of porewater salinity, pH and ORP changed significantly with mangrove ages in both seasons in the wet season, ($p < 0.05$, Fig. S1), except for porewater salinity at the bare sediment during the dry season. The deeper layers of each sediment core (>10 cm) did not exhibit much variability in their properties. Minimum pH was recorded at the top 10 cm depth of the mature mangroves in the wet

Formatted: Superscript

280 season (5.41±0.265-23). Vertical profiles of TOC and $\delta^{13}\text{C}$ showed wide variations than the physico-chemical properties (Figs. 3a-d). Notable peaks for TOC were observed in mature mangroves (6 cm and 25 cm in dry and wet season, respectively) and adult mangroves (20 cm; dry season). Total organic carbon and $\delta^{13}\text{C}$ in bare sediment changed very little with depth especially in the dry season. Significant differences in OC/TN molar ratios between sediment from different depth of MM and other sites were observed (Fig. 3e,f). At the non-vegetated site (BS), the ratios varied slightly with seasonal changes. The vertical profile of SSA based on the values at three specific depths of each core showed a mild decreasing trend from the surface to the deepest layer (50 cm) in both dry and wet season (Figs. 4a,b). The depth-specific values of SSA were always higher at the adult mangrove sites than the other two (except at 45-50 cm in the dry season). Similar to SSA, OC loading also decreased with core depth and mature mangrove exhibited maximum loading in both seasons (Figs. 4c,d). All stages of mangrove development showed an overall increase of DOC concentration with depth regardless of the seasons (Fig. 5a-b). DOC concentrations of deeper layers reached up to four to five times higher than those of the upper sediment in the wet season and two to three times higher in the dry season. For example, our data demonstrated a change from 600 to around 4000 $\mu\text{mol L}^{-1}$ DOC concentrations for the adult mangrove in both the dry and wet season. A wide range in DOC of 128 to 920 $\mu\text{mol L}^{-1}$ was also noticed for the non-vegetated bare sediment site.

295 On the basis of Using the generalized additive model (GAM) as the basis, the results of ANOVA for the main parameters showed significant dependence of TOC over mangrove types ($F = 46.37$, $p < 0.001$), and depth ($F = 9.80$, $p < 0.001$) (Table 1). Porewater DOC varied significantly with mangrove types ($F = 4.42$, $p < 0.005$), similar to the $\delta^{13}\text{C}$ ($F = 28.3$, $p < 0.001$) and $\delta^{15}\text{N}$ ($F = 3.92$, $p < 0.05$). The coefficients in each parameter based on the GAM for TOC, DOC and $\delta^{13}\text{C}$ are given in Table S2 and their changes with depth as smooth term are shown in Fig. S2.

300 The OC/TN and $\delta^{13}\text{C}$ of the five mangrove types were plotted with the four end-member sources (River POM, Marine POM, Leaf and MPB) to rectify sources of SOM (Table 2, Fig. S3) Fig. 6), and subsequently calculate end-member contribution to each type (Fig. 7, Table 2, Fig. S3 Table S3). Except for MPB and marine POM, the relative contributions of mangrove leaf and river POM were significantly different for each site (one-way ANOVA, p-value mangrove leaf <0.05, p-value river POM <0.05). At the bare sediment and pioneer mangrove sites, River POM dominated the SOM pool with maximum contribution of 58.80% and 43.75%, respectively, whereas at the young and mature stands, mangrove leaf was the main potential contributor (57.3% and 58.82%, respectively). On the other hand, SOM remained more as a mixture of river POM and leaf material (~60.40%) at the adult mangrove sites. The contributions of benthic and pelagic algae as SOM sources were not very significant for the entire mangrove sediment in the area studied.

310 In the water part, results from three locations (upstream-channel-offshore) showed salinity changing from 0 to 33, pH increasing from 7.6 to 8.1, and DO (%) increasing from 89% to 105% to the downstream (Table S4). Surface water POC was 4-5 fold lower than the DOC in the upstream and channel water (~ 20 $\mu\text{mol L}^{-1}$ $\mu\text{mol L}^{-1}$ versus 90 $\mu\text{mol L}^{-1}$ $\mu\text{mol L}^{-1}$), and lowest in offshore water (10 $\mu\text{mol L}^{-1}$ $\mu\text{mol L}^{-1}$). The $\delta^{13}\text{C}$ -POC was highest in offshore water (-22.8‰) and lowest upstream (-25.9‰).

4. Discussion

315 **4.1 Relevance of chrono-sequence approach**

Several studies have relied on direct measurement of carbon accumulation rates (CAR) by combining sedimentary C content and soil accumulation rates estimated from radioisotopes, ^{210}Pb and ^{137}Cs or natural markers like volcanic ashes (Sanders et al., 2010). These CAR estimations are based on the assumption that sediment and OC accumulation are in a steady state during the period of accumulation/deposition. However, the "indirect way" or the chrono-sequential theory assumes that the temporal variations in soil properties in different aged sites fall into the same time trajectory of OC accumulation. This assumption requires a condition that these different sites had experienced similar driving factors of OC accumulation processes following tree growth after the restoration. While hydrological processes such as hydroperiod and tidal regime are considered to be one of the important drivers of OC accumulation, it is regarded that considered that these conditions do not largely vary among the sites and have been relatively stable over the time window in concern (~ 30 years after restoration) given the same level of ground elevations which located in the same forest (Fig. 2). Also, given the significant fraction of mangrove contribution to SOC (Table 2 Fig. 7), the influence of C inputs from external systems may not be a significant factor in shaping the OC accumulation trajectories in the sites. Only the vegetation structures vary significantly among sites that may characterize the evolution of OC stocks with forest age in our study site, Bakhawan Ecopark (Fig. 87). In addition, we consider that the AGB and BGB development in the sites follow a similar trajectory given the same level of soil salinity (Fig. 2) – one of the most important regulators of mangrove growth, and the same plantation spacing and species. Therefore, it is reasonable to consider that the OC accumulations in the different aged sites also follow the similar time trajectory, and thus Eq. (3) can be applied to estimate CAR in our study site.

335 **4.2.1 Sediment condition and organic matter**

The results of dry bulk densities and granulometry (coarse fraction, SSA,) of the tidal flat and mangroves in Bakhawan Ecopark indicate that soils are relatively homogeneous with fine-grained fractions relatively prevalent towards the upper older mangroves at higher elevation-region (mainly towards AM), while towards the shore, coarse-grained sands are more common on the tidal flat and younger mangroves (BS and YM, PM) (Fig. 2). Bulk densities (BD) at the sampling sites (0.3 to 1.3 g cm⁻³) were comparable higher than with the reported BD values across mangrove soils of the Indo-Pacific regions (0.20 to 0.92 g cm⁻³; Donato et al., 2011), with sand fractions dominating the lower intertidal zone. Specific surface area is primarily constrained by grain size and its vertical profile is presumably related to finer upward trend of sediment grain (Fig. 4a, c). The latter might have been a result of sediment-stabilizing function of mangroves or influenced by weathering process that transforms sand and silt fractions into clay fractions, some land use change in recent years (e.g., land use change can increase clay content via deposition of pollen, (Shen et al., 2020). Furthermore, carbonate bearing minerals can influence SSA more on the tidal flat than the organic rich mangrove sediment. Among the older stands (MM and AM), higher SSA and sediment thickness, and low BD at the adult stands suggest dominance of finer-grained clay material probably because of the long-term deposition of the weathered minerals, long-term presence of mangrove itself, and the narrow sandbar halfway down the Ecopark (Fig. 1) that may have closed off the older mangroves from higher wave energy and shifted deposits of finer grains. Total organic carbon

Formatted: Font: (Default) Times New Roman, 10 pt

is higher at the older sites than the younger ones due to such fine-grained (silt + clay) sediments that tend to have higher TOC than the coarse sands (Canfield, 1994). Fine-grained silt has larger SSA that create higher capacity to adsorb OM (Mayer, 1994).

Among the physicochemical properties, lower porewater salinity at the BS than the mangrove sites indicate greater dilution from direct input of river water, which become less with increasing elevation level inside the forest floor (Fig. 2). On a temporal scale, overall low porewater salinity during the wet season is more likely linked to rainwater dilution (350-450 mm in September, 75-150 mm in February; JRA-55 Reanalysis) and elevated groundwater level. Because of shading effect, surface sediment temperature at the mangrove vegetated sites was lower than the sun-exposed BS or PM. The lowest recorded ORP at BS was due to reducing conditions that prevailed through tidal water saturation, strongly suggests that exchange of porewater with overlying water is limited, and this may have implication on the interpretation of porewater chemistry (i.e., DOC, section 4.3).

It has been observed that mangrove sediments in the river-dominated estuary accumulate larger proportion of the mangrove-derived OM than those in the tide-dominated estuaries/oceanic mangroves dominated by marine algae (e.g., Indonesian mangroves, Kusumaningtyas et al., 2019; Latin American, Gonharet et al., 2014; Middle-East, Ray and Shahraki, 2016). In the microtidal riverine setting of the Bakhawan Ecopark, OM input from land sources is more dominant than the marine sources at the mangrove sites (Fig. 6). End-member mixing model suggests that there is a clear gradient with respect to the relative proportion of OM sources along the tidal flat-mangrove continuum (Fig. S37).

Sediments from cores at the bare sediment and pioneering mangrove sites show the predominance of OM probably derived from fluvial transport of eroded organic material within the catchment. Upon transport into the coastal area, fine sediment and POM accumulate in calm shallow water channel at the topographically lowest elevation zone, (Fig. 2) and consequently the longer inundation period facilitates sedimentation and deposition of the suspended matter. Similar values of $\delta^{13}\text{C}$ in surface water POC upstream (~25.9‰, Table S3) and sediment OC at the bare sediment and pioneering mangroves (mean ~26‰) support their upstream allochthonous sources. A sizeable contribution from MPB may not be ruled out at bare sediment despite its minimal contribution from the mixing model (Fig. 7). A sizeable fraction of OC at the tidal flat was contributed by the marine and benthic algae. In a companion study, other than the visible evidence of green algal patches, the measured day-time CO₂ uptake flux on the tidal flat, which contrasts with the emission flux at the forested sites (tidal flat: ~4 to ~2 mmol m⁻² h⁻¹, mangrove: 5–12 mmol m⁻² h⁻¹, Ray et al., unpublished). Strikingly low OC:TN ratio at the surface sediment and minimum $\delta^{15}\text{N}$ suggests presence of N₂ fixing bacteria on the tidal flat during exposed tide condition. The slightly higher mangrove contribution to SOM in pioneering mangroves (up to ~54%) clearly indicates additional OM input from the small growing plants along the channel.

At the topographically higher mangrove sites, greater contributions of autochthonous sources (i.e., mangrove plant materials) are correlated with lower $\delta^{13}\text{C}$ and higher OC/TN (>12). This is favored by the relatively high bed elevation and decrease in submersion time, promoting the retention of detrital OM in the sediment layer (shown as leaf OM, Fig. S37). Although such evidence of greater plant input to SOM at interior mangrove sites compared to mudflats are

not new for the intact forests (Marchand et al., 2003; Sanders et al., 2010; Matos et al., 2020), this is rare for restored mangroves considering an extended gradient from mudflat to mangrove appearance (except in Vietnam³⁵; Van Hiew et al., 2017).

390 Terrestrial C3 vascular plants, like mangrove plant organ have C/N ratios of around 12 or higher (Prahl et al., 1980) as it is composed predominantly of lignin and cellulose, which are nitrogen-poor. The significant positive correlation between TOC and TN ($r^2 = 0.96$ at BS, PM, YM, and AM; $r^2 = 0.42$ at MM, figure not shown) in the sediments indicate that the C and N in the samples are predominantly associated with the organic pool. [This suggests the protective role of early mangrove recruitment on sedimentary organic matter as seen in European coastal wetland \(Jiménez-Arias et al., 2020\)](#). It is noteworthy that such correlation is relatively poor at the mature stands. Although the exact reason for this is unknown, the abundance of benthic animals during another complimentary experiment (burrow density at MM: 150 ± 55 , YM: 70 ± 62 , BS: 5 ± 2 individual m^{-2} , Ray et al., unpublished) might suggest intense bioturbation and sediment remobilization.

Formatted: Superscript

4.32 Vertical profile of organic carbon

400 [The variation in OC content from the bottom to the top of sediment cores also reflected the change in the proportion of mangrove-derived materials and allochthonous \(e.g., benthic algae\) organic carbon sources in the sediments and the mineralization of organic matter in the mangrove sediment \(Tue et al., 2011\)](#). The difference in the sediment physicochemical and OC profile at the upper 50 cm of the layers may result from multiple factors that promote OM decomposition, such as immediate exposure of litter in surface layers (e.g., managed *Rhizophora* in Malaysia, Ashton et al., 1999), while coarse and fine roots contribute to carbon and nutrients at shallower depth³⁶ (reported down to 52 cm for 27-yr³⁷ planted *Rhizophora* in Vietnam³⁸; Arnaud et al., 2021). Multiple mid-layer peaks of TOC are sometimes observed which presumably reflects the influence of root biomass (Fig. 3). This study showed that root activity within the sediment column is essentially dominant when comparing vegetated sites with bare sediment. Assuming a mixture of algae (marine POM plus MPB, $\delta^{13}\text{C} = -21.07\text{\textperthousand}$), and mangrove root/plant organ ($\delta^{13}\text{C} = -28\text{\textperthousand}$) as two major end-member sources of the sediment OM pool, provenance analysis confirms that roots contribute maximum at the old stands (75–100%) and minimum at BS and PM (52–72%) corroborating to the TOC peaks observed at different depths (particularly between 10–25cm, Fig. 3a, b). [This has been shown in other studies that root-derived carbon tends to be accumulated more efficiently as aggregates in SOM pool and contribute largely as potential C source \(Xia et al., 2005\)](#).

Formatted: Font: (Default) Times New Roman, 10 pt

Formatted: Font: (Default) Times New Roman, 10 pt

Formatted: Font: (Default) Times New Roman, 10 pt

Formatted: Font: 10 pt

415 [Organic carbon profile](#) Depth-wise patterns of OC were not much variable ~~was almost uniform~~ in both seasons (Figs. 3a, b) suggesting a dominant OM source prevail~~inged~~ down the cores. Root exudates like sugars, ~~and~~ amino acids are suggested to be the main carbon source for the localized microbes (Bouillon and Boschker 2006; Jiang et al., 2017). [As mentioned in the previous section, bioturbation might play an important role in carbon accumulation at the shallow sediment depth of the older stands where maximum burrow densities were observed compared to the tidal flat and younger mangrove sites.](#) The role of burrowing crabs as carbon sink has also been reported at deeper soil layers of *Avicennia* stands in Kenya (40–80 cm, Andreetta et al., 2013) where burrowing sesarmids provide a continuous supply of fresh organic matter down the profile. At low tide, ~~the~~ presence of water with low oxygen saturation, covering the

425 bottom of the burrows avoids oxidation by creating an extension of sediment-air interface and favoring greater OC concentration where crab population were maximum., otherwise hypoxic- or anoxic, and create an extension of coastal marshes sediment-air interface favoring greater OC accumulation. In this study, bioturbation might play an important role in carbon accumulation at the sediment horizon of the older stands where higher benthic communities were found compared to the tidal flat and younger mangrove sites.

430 The depth-wise relationships between sediment OC and porewater DOC are less obvious (Fig. 3, 5). Porewater DOC varies disproportionately with OC. The distinct feature of vertical DOC profile is the non-uniform distribution of concentration with mangrove age in contrast with the relatively uniform profile at the bare sediment. Porewater DOC in non-vegetated sediments is known to be primarily controlled by oxygen availability and the presence of microphytobenthos that could drive porewater dynamics via OC leaching compared to mangrove sediments. At the vegetated sites, fluorescence and hydrophobic DOC of high molecular weight is known to drastically increase in 435 anoxic coastal porewaters (Komada et al., 2004; Marchand et al., 2006). At the vegetated sites, porewater DOC concentrations showed higher concentrations with depth that is most likely a reflection of the net effect of diagenesis, subsurface transport and partial control via root uptake and release. Low surface DOC might be the reason of higher mixing and dilution with overlying water of low DOC concentration (Table S1). Though the salinity profile is not exactly like DOC, yet the salinity peaks at the sub surface depth, thereby creating a uniform pattern followed at AM 440 and MM. This may lead us to the hypothesis that water absorption by roots at the upper sediment may be augmented by the presence of radial mangrove roots leading to an increase of salinity at some sites and gravitational percolation of salt water and DOC to greater depths. However, unlike porewater salinity that is lower in the wet season than dry season due to rainwater dilution, DOC did not vary seasonally at adult mangrove and mature mangrove sites suggesting perennial source and retention in the sediment. The porewater profile of salinity and DOC in mangrove 445 sediments is very rare in the literature. One such comprehensive dataset by Marchand et al. (2006) in the French Guiana reported similar findings of higher DOC at greater depth with mangrove ageing but no direct correlation with other co-variables. Like shown many years ago by Marchand et al. (2006), the influence of seasonal- mangrove productivity and root activity on the DOC vertical profile may be evident also for this study, however, detailed research is necessary to understand such relationship.

450 **4.43. Increase of organic carbon with mangrove development**

The average TOC concentration in the top 50-cm mangrove sediments (PM to MM) in Bakhawan Ecopark is lower (2.5±1.8 $\mu\text{mol mg}^{-1}$) than the Indo-Pacific regions (9.9±5.2 $\mu\text{mol mg}^{-1}$; Donato et al., 2011) but comparable with the global mean (1.7 $\mu\text{mol mg}^{-1}$; Kristensen et al., 2008) and other restored mangroves in SE Asia (e.g., 2.2±0.05 $\mu\text{mol mg}^{-1}$ in Vietnam; Dung et al., 2016) and China (4.2±0.3 $\mu\text{mol mg}^{-1}$; Nam et al., 2016). The Absence of peat organic layer at the sampled sites and fast decomposition observed in separate CO_2 emission measurement (benthic emission: 8 $\text{mmol m}^{-2} \text{hr}^{-1}$ nearly at the upper limit of global range 0.25 to 10.4 $\text{mmol m}^{-2} \text{hr}^{-1}$, Bouillon et al., 2008, Ray et al., unpublished) are the possible reasons behind such low to moderate OC in sediment. Besides this, that, the rapid flushing out of POC favored by the low-lying gentle elevation could account for the OC-poor state of the system.

Formatted: Not Superscript/ Subscript

460 Isotope evidence of POC further indicate that it was sourced from the eroded mangrove soil composed of litter debris (mean around -25.0‰ for salinity 0–25, Table S4) coming from the upstream and mangrove sites that flushes water away via the channel to the offshore (-25.0‰ at salinity 33) at ebb tide-time.

465 The present result shows that the development of restored mangrove forests could improve sediment OC as indicated by a clear progression in sediment TOC among the planted mangroves of different developmental stages leading towards soil maturity. The accumulation of OC in the mangrove sediments may be attributed to the increases in belowground root expansion with stand age (Salmo et al., 2014). Because of restricted water exchange with the seawater, mature *Rhizophora* stands accumulate higher mangrove derived OM (leaf litter and decomposing fine roots) than the young and pioneering stand, therefore showing higher TOC. For the adult mangrove stands (AM) despite their moderate biomass, oxic conditions (positive ORP) may have favored OM decomposition in the wet season resulting into lower TOC than at MM. Such non-linear correlation of OC with mangrove chrono-sequence is in line 470 with other works in the restored (Lunstrum and Chen, 2014; Van Hiew et al., 2017) and intact forests (Lovelock et al., 2010; Marchand et al., 2017).

475 Like TOC concentration, OC stocks in sediments gradually increased with chrono-sequence which is consistent with other recent studies on mangrove plantations (Lunstrum and Chen, 2014; Van Hiew et al., 2017; Wang et al., 2021). Salmo et al., (2013) previously reported higher above ground biomass (AGB) in 17-yr old *Rhizophora* than the 12-yr old stands (101.8 versus 51.4 Mg ha^{-1}) at the Bakhawan Ecopark. Fine root production has also been found to increase with AGB and contribute to sediment OC stocks more in mature mangroves (Zhang et al., 2021). On a global basis, OC stocks are mostly reported for sediment cores of 1 m depth. If core depth is normalized to 50 cm, our results still give comparable estimates (3 to 77 Mg C ha^{-1}) to the limited assessments of the restored mangrove park (Table 3), such as in north central Vietnam (54 to 84 Mg C ha^{-1} , 0 to 27 yrs of *Kandelia obovata*; Van Hieu et al., 2017), 480 Pichavaram (41 to 94 Mg C ha^{-1} , 12 to 21 yrs of *Rhizophora spp.* (Gnanamoorthy et al., 2019) and Bhitarakanika Conservation in India, (38 Mg C ha^{-1} , 5 yrs *Kandelia candel*, Bhomia et al., 2016). However, our stock estimate is lower than the organic soil of oceanic setting in Sulawesi, Indonesia (c.a. 150 – 300 Mg C ha^{-1} , more than 10 years of *R. apiculata*, Cameron et al., 2019). Sediment OC stock is largely dependent on vegetation biomass and extent of litter input. Salmo et al., (2014) reported that 17- and 18-year old *Rhizophora* stands at the Bakhawan Ecopark had 30 – 40 % lower AGB compared with the natural mangroves (150 ton ha^{-1}) while 50-year old stands had similar AGB (132 ton ha^{-1}) with natural mangroves. Another reason might be the river dominated mangrove settings which are known to transport high allochthonous input and deposit mineral sediment that dilutes OM and lowers OC stocks than the marine settings where mangrove-derived OM increase carbon stocks in the sediment (Jennerjahn, 2020). Another reason could be the sediment reworking during restoration or plantation work that can mobilize OC at least from the 485 top 10 cm of the sediment. The rapid turnover may lead to reduction in OC stocks. From a more general perspective, sediment OC stocks depends on the distribution of fine roots at the adult sites (Noguchi et al., 2020) and roots generally have lower decomposition rates than leaves favoring C storage partly because of the composition relatively rich in recalcitrant material such as suberin and lignin root-derived C (Rasse et al., 2005), and efficient redox-dependent

490 Formatted: Font: (Default) Times New Roman, 10 pt

Formatted: Font: (Default) Times New Roman, 10 pt

Formatted: Font: 8 pt

decay processes like sulfate reduction that promote OM preservation and increase OC stock in older stands isolated from the sea (Lambs et al., 2008).

The increase in porewater DOC concentrations observed from tidal flat to pioneer mangrove then to the older mangrove seems to reflect the increasing pattern of bulk OC (Fig. 2). With greater biomass, (mean tree height: PM <1m, YM 3-4m, AM 6-8m, MM 10-15m, data not shown), sediment TOC and porewater DOC concentration successively increased, the latter due to greater leaching of the sizable SOM with age. A similar trend for bulk and dissolved OC was observed in the naturally growing *Avicennia* dominated mangroves in the Amazonian coastline (Marchand et al., 2006). With the progression of chrono-sequence, we may infer that the higher the biomass, the higher the TOC, and the higher the DOC concentrations in the shallow sediments.

Organic carbon preservation in marine sediments can be influenced by the physical factors such as association of OC with the surface of sediment mineral particles, also known as OC loading (Kiebel and Mayer, 2014). Sediments with high SSA tend to be rich in clay, iron and aluminum and store greater amounts of OM than low-SSA soils due to intimate organo-mineral association (Mayer, 1994). Therefore, OC loading can be considered as a proxy for blue carbon preservation and supply in the marine system, although there has been no account of such result for mangroves worldwide. Our estimates of OC loading for the mangrove sediments and tidal flats (mean: 152 and 25 $\mu\text{mol C m}^{-2}$) are within the range of marine and costal observations (Table 3), continental margin sediment (40-80 $\mu\text{mol C m}^{-2}$, Mayer, 1994), vegetated marine sediment (56-67 $\mu\text{mol C m}^{-2}$, Miyajima and Hamaguchi, 2017), and floodplains (16-42 $\mu\text{mol C m}^{-2}$, Goni et al., 2014), but much lower than in the high altitude soils where mineral phases are fully covered by rich-OM with high OC% (300-780 $\mu\text{mol C m}^{-2}$, 5 to 10%; Wagai et al., 2009). At the Bakhawan Ecopark, the variability of OC loading between mangrove sediments and tidal flat can be explained by the difference in spatial extent of the individual sampled site. For example, when SSA is greater than 15 $\text{m}^2 \text{ g}^{-1}$ (at AM and MM), significant negative correlation was observed between OC and SSA ($r^2 = 0.95$, $p < 0.01$, $n = 7$, figure not shown) indicating that the net accumulation rate of OC in these sites are not dependent on mineral particles but on the mangrove-derived supply of OM. Whereas at BS with mean SSA <15 $\text{m}^2 \text{ g}^{-1}$, a quasi-significant positive relationship between these two variables suggests the possible role of physical sorption of OC in the riverine sediment mineral matrices for stabilization and sequestration of organic carbon ($r^2 = 0.50$, $n = 6$). Therefore, the sediments in the mangroves does not share a common OC sequestration mechanism as with the pelagic continental shelf and seagrass sediments.

4.4 Accumulation of organic carbon

4.4.1 Relevance of chrono sequence approach

Several studies have relied on direct measurement of carbon accumulation rates (CAR) by combining sedimentary C content and soil accumulation rates estimated from radioisotopes, ^{208}Pb and ^{137}Cs or natural markers like volcanic ashes (Sanders et al., 2010). These CAR estimations are based on the assumption that sediment and OC accumulation are in a steady state during the period of accumulation/deposition. However, the "indirect way" or the chrono-sequential theory assumes that the temporal variations in soil properties in different aged sites fall into the same time

530 trajectory of OC accumulation. This assumption requires a condition that these different sites had experienced similar driving factors of OC accumulation processes following tree growth after the restoration. While hydrological processes such as hydroperiod and tidal regime are considered to be one of the important drivers of OC accumulation, it is considered that these conditions do not largely vary among the sites and have been relatively stable over the time window in concern (~30 years after restoration) given the same level of ground elevations which locate in the same forest (Fig. 2). Also, given the significant fraction of mangrove contribution to SOC (Fig. 7), the influence of C inputs from external systems may not be a significant factor in shaping the OC accumulation trajectories in the sites. Only the vegetation structures vary significantly among sites that may characterize the evolution of OC stock with forest age in our study site, Bakhawan Ecopark (Fig. 8). In addition, we consider that the AGB and BGB development in the sites follow a similar trajectory given the same level of soil salinity (Fig. 2) – one of the most important regulators of mangrove growth, and the same plantation spacing and species. Therefore, it is reasonable to consider that the OC accumulations in the different aged sites also follow the similar time trajectory, and thus Eq. (3) can be applied to estimate CAR in our study site.

535

540

4.4.2 Carbon sink capacity

545 The burial of OC in the sediment strongly depends on many environmental conditions such as mangrove forest productivity, deforestation and degradation rate, sediment accretion, topography, tidal regime, and bioturbation activities (Alongi, 2014; Pérez et al., 2018). Significant exponential and/or linear increase of OC stock with early mangrove age (until 4 YM) could be the result of longer time duration since the early colonization of plants (Fig. 7a), probably suggests that primary productivity might be key controlling factor for C accumulation (Fig. 8a). However, the correlation between the standing stock of sediment OC with ageing at the adult/matured stands are essentially not very significant, indicating that the size of the sediment OC pool at these two sites are not determined 550 simply by the primary production of the vegetation but is also might be constrained significantly by some other biological or geophysical factors. The rates of OC accumulation defined by their respective slopes in the exponential curve (BS to MM) and linear curve (YM to MM) at individual site of 50 cm depth (5.9 – 33 mol m⁻² yr⁻¹, and 15.93 mol m⁻² yr⁻¹, respectively, Figs. 87a,b) are well within the ranges by chrono-sequential analysis of 1m cores in restored (12.7 mol m⁻² yr⁻¹, Lunstrum and Chen, 2014), conserved (14 mol m⁻² yr⁻¹, Pérez et al., 2018), intact (6 to 40 mol m⁻² yr⁻¹, Marchand et al., 2017), or encroaching mangroves (19 mol m⁻² yr⁻¹, Kelleway et al., 2016). System specific variabilities such as sedimentation rate, decomposition rate, rate of litterfall and root production may cause such 555 differences in CAR among the reported mangroves. It is noted that OC% in other reported for the mangrove soils were on average 2 times higher than the Bakhawan sites due to high terrestrial input to this forest driven by historical land use changes.

560 4.55 Implication of blue carbon chrono-sequence

There is a crucial need to improve scientific understanding on blue C dynamics and to develop an appropriate framework for blue C assessment and monitoring mechanisms for future policy development. Achieving improved scientific understanding on C sources and stocks and to monitor the changes in accumulation rate at the early development stage and adult stages of mangrove stands would require practical tools and guidance to enable the

565 conduct of proper C analyses. In this study, the supply of OM from the mangrove vegetation, benthic algae and upstream sediment transport are recognized as controls of blue C at the mangrove sites and tidal flat. Impression of more mangrove-derived C input is evident with mangrove development. Such apportionment of OC sources at different mangrove stand ages should be useful to improve our future knowledge on the origin of blue C in REDD+ accountings that is yet to register sedimentary OC within the reduced C emission scheme despite sediment being
570 recognized as the largest C pool in the mangrove ecosystem (Duarte et al., 2013). A prior knowledge on sources and character of OC (generally refractory or mangrove-derived and labile or algal-derived) would be beneficial for fostering mangrove plantation programs. Greater mangrove-derived OC accumulation with ageing at the Bakhawan Ecopark might suggest long term storage of the refractory fraction, hence an effective return to REDD+ strategy.

575 Another perspective is that any attempt of quantifying OC stock and accumulation rate following a plantation program should be well recorded in the relevant carbon accounting programs. For example, the Verified Carbon Standard Methodology (www.verra.org) existing for mangrove restoration projects that is certified under the Cleaner Development Mechanism (CDM) program of the United Nations Framework Convention on Climate Change (UNFCCC, 2011) assumes CAR for 0–20 years mangrove as $4 \text{ mol m}^{-2} \text{ yr}^{-1}$ after plantation (Lunstrum and Chen, 2014), which is 4 times lower than our chrono-sequence based estimate ($\sim 16 \text{ mol m}^{-2} \text{ yr}^{-1}$, linear slope for YM to MM stands, figure not shown). For the Bakhawan Ecopark having mangrove coverage of 121 ha, total organic carbon stock and accumulation rate in the vegetated soil are estimated to be 2795 to 11500 Mg C ha⁻¹, and 72 to 304 Mg C yr⁻¹, respectively. Carbon stock in the above-ground biomass was 2744 to 5499 Mg C ha⁻¹ for the younger and adult sites (derived from the literature data by Salmo et al., 2014, using biomass to C conversion factor of 45% from IPCC 2013). However, if the IPCC default values are used to compute total C stock in sediment and above-ground biomass (386, and 92-192 Mg C ha⁻¹, respectively), significant differences can be observed between the observed and computed results as 5009 to 10454, and 46700 Mg C ha⁻¹, respectively. Given the IPCC default values are derived from the intact forest while our observed data were taken from restored sites, such direct comparison has potential biases. Similar discrepancies are also present for emission fluxes, such that in IPCC Tier 1, where In IPCC 2013 supplementary (Tier 1, chapter 1), default CO₂ emission factor from tidal flat was set to be 0, while it was $-14 \text{ mol m}^{-2} \text{ yr}^{-1}$ (negative means accumulation) for the planted/rehabilitated mangroves, the latter is in line with the older mangroves at Bakhawan Ecopark, but not with each developmental stage. Such assumption may lead to severely underestimated actual blue carbon sink capacity of the mangroves and consequently carbon emission value. Therefore, a differential yet steady trend of blue C potential based on short-term chrono-sequence can help define the utility of a mangrove restoration efforts.

595 5. Conclusion

600 This study is a first attempt to apply a chrono sequence (or space-for-time substitution) approach to evaluate the distribution and accumulation rate of carbon in a 30-year old (maximum age) restored mangrove forest. From this study, it is clearly seen that mangrove tree development coincided with sediment OC concentration and accumulation, hence mangrove plantations are expected to accelerate OC sequestration at the early plantation stage. Source apportionment of sedimentary OM suggests higher contribution of mangrove vegetation at higher elevations upland

Formatted: Superscript

Formatted: Superscript

Formatted: Superscript

and riverine POM plus benthic algae down the tidal flat. The accumulation of OC in the sediment may be attributed to the increases in belowground root expansion with stand age. This chrono-sequence based estimates of OC stock and accumulation rate can be useful reference for setting up carbon accounting in *the Rhizophora*-dominated mangrove restoration projects.

605

Acknowledgement

We are grateful to the Japan International Cooperation Agency (JICA) and Japan Science and Technology Agency (JST) through the Science and Technology Research Partnership for Sustainable Development Program (SATREPS) for financially supporting the Project “Comprehensive Assessment and Conservation of Blue Carbon Ecosystems and 610 their Services in the Coral Triangle (Blue CARES)”. We thank Jesus Abad, John Michael Aguilar, Dominic Bautista, Bryan C. Hernandez and Mr. Tsuyoshi Kanda for their assistance during field surveys. We are grateful for the overall support given by the University of the Philippines, Diliman and Aklan State University to the project. We are thankful to our BlueCARES colleague Dr. Charissa Ferrera for supporting in language edits throughout the manuscript. Finally, authors sincerely thank reviewers for their constructive comments that have greatly improved the revised version.

615

Competing interests

The authors declared no potential conflict of interests.

620 **References**

Alongi, D.M: Carbon cycling and storage in mangrove forests, *Ann. Rev. Mar. Sci.* 6, 195–219, doi: 10.1146/annurev-marine-010213-135020, 2014.

Alongi, D.M.: Global Significance of Mangrove Blue Carbon in Climate Change Mitigation, *Sci.* 2, 67, doi:10.3390/sci2030067 2020.

625 Alongi, D.M., Sasekumar, A., Chong, V.C., Pfitzner, J., Trott, L.A., Tirendi, F., Dixon, P., and Brunsell, G.J.: Sediment accumulation and organic material flux in a managed mangrove ecosystem: estimates of land–ocean–atmosphere exchange in peninsular Malaysia, *Mar. Geo.*, 208, 383–402, doi:10.1016/j.margeo.2004.04.016, 2004.

Ashton, E.C., Hogarth, P. J., and Ormond, R.: Breakdown of mangrove leaf litter in a managed mangrove forest in 630 Peninsular Malaysia, *Hydrobiologia*, 413: 77–88, 1999.

Arnaud, M., Morris, P.J., and Baird, A.J.: Fine root production in a chronosequence of mature reforested mangroves, *New Phytologist*, doi: 10.1111/nph.17480., 2021.

Andreetta, A., Fusi, M., Cameldi, I., Cimò, F., Carnicelli, S., and Cannicci, S.: Mangrove carbon sink, Do burrowing crabs contribute to sediment carbon storage? Evidence from a Kenyan mangrove system, *J. Sea Res.*, 85: 524-533, doi: 10.1016/j.seares.2013.08.010, 2014.

Bhomia, R.K., MacKenzie, R.A., Murdiyarso, D., Sasmito, S.D., and Purbopuspito, J.: Impacts of land use on Indian mangrove forest carbon stocks: implications for conservation and management, *Ecol. Appl.*, 26, 1396e1408, doi: 10.1890/15-2143, 2016

Brown, R.D., Marotta, H., and Peixoto, R.B.: Hypersaline tidal flats as important “blue carbon” systems: a case study from three ecosystems, *Biogeosciences*, 18, 2527–2538. doi: 10.5194/bg-18-2527-2021, 2021.

Boto, K.G., and Wellington, J.T.: Soil characteristics and nutrient status in a Northern Australian mangrove forest, *Estuaries*, 7, 61–69, doi: 10.2307/1351957, 1984.

Bouillon, S., and H. T. S. Boschker.: Bacterial carbon sources in coastal sediments: a cross-system analysis based on stable isotope data of biomarkers, *Biogeosciences*, 3, 175–185, doi: 10.5194/bg-3-175-2006, 2006.

Cadaweng, E. A. and Aguirre, J. A.N.: Forest from the mud: the Kalibo experience. in: *In Search of Excellence: Exemplary Forest Management in Asia and the Pacific*, edited by: P.B. Durst, C. Brown, H.D. Tacio and M. Ishikawa, Bangkok, Thailand: FAO, 39-48, 2005.

Cameron, C., Hutley, L.B., Friess, D.A., et al.: Community structure dynamics and carbon stock change of rehabilitated mangrove forests in Sulawesi, Indonesia, *Ecol. Appl.*, 29, e01810, doi: 10.1002/eap.1810, 2019.

Chen, J., Wang, D., Li, Y., Yu, Z., Chen, S., Hou, X., White, J.R., and Chen, Z.,: The carbon stock and sequestration rate in tidal flats from coastal China, *Global Biogeochem. Cy.*, 34(11), p.e2020GB006772, doi: 10.1029/2020GB006772, 2020.

Donato, D.C., Kauffman, J.B., Murdiyarso, D., Kurnianto, S., Stidham, M., and Kanninen, M.: Mangroves among the most carbon-rich forests in the tropics, *Nature Geosci.*, 4: 293-297, doi: 10.1038/ngeo1123, 2011.

Dung, L.V., Tue, N.T., Nhuan, M.T., and Omori, K.: Carbon storage in a restored Mangrove forest in Can Gio Mangrove Forest Park, Mekong Delta, Vietnam, *Forest Ecol. Manag.*, 380, 31–40, doi: 10.1016/j.foreco.2016.08.032, 2016.

Duarte, C.M., Losada, I.J., Hendriks, I.E., Mazarrasa, I., and Marbà, N.: The role of coastal plant communities for climate change mitigation and adaptation, *Nature Climate Change*, 3(11): 961-968, doi: 10.1038/nclimate1970, 2013.

Duncan, C., Primavera, J.H., Pettorelli, N., Thompson, J.R., Loma, R.J.A., and Koldewey, H.J.: Rehabilitating mangrove ecosystem services: A case study on the relative benefits of abandoned pond reversion from Panay Island, Philippines, *Mar. Pollut. Bull.*, 109(2): 772-782, doi: 10.1016/j.marpolbul.2016.05.049, 2016.

665

[Elwin A., Bukoski, J.J., Jintana, V., Robinson, E.J.Z., Clark, J.M.: Preservation and recovery of mangrove ecosystem carbon stocks in abandoned shrimp ponds. Sci Rep. 4, 9:18275. doi: 10.1038/s41598-019-54893-6, 2019.](#)

Formatted: Font: (Default) Times New Roman, 10 pt

Formatted: Font: (Default) Times New Roman, 10 pt

Formatted: Font: (Default) Times New Roman, 10 pt

670

Gnanamoorthy, P., Selvam, V., Ramasubramanian, R., Chakraborty, S., Pramit, D., and Karipot, A.: Soil organic carbon stock in natural and restored mangrove forests in Pichavaram south-east coast of India, Indian J. Geo-Mar. Sci., 48, 2019, 801-808, 2019.

675

Gontharet, S., Mathieu, O., Lévéque, J., Milloux, M.J., Lesourd, S., Philippe, S., Caillaud, J., Gardel, A., Sarrazin, M., and Prousy, C.: Distribution and sources of bulk organic matter (OM) on a tropical intertidal mud bank in French Guiana from elemental and isotopic proxies, Chemical Geology, 376: 1-10, doi: 10.1016/j.chemgeo.2014.03.009, 2014.

675

Goni, M.A., Moore, E., Kurtz, A., Portier, E., Alleau, Y., and Merrell, D.: Organic matter compositions and loadings in soils and sediments along the Fly River, Papua New Guinea, .Geochim. Cosmochim. Ac., 140: 275-296, doi: 10.1016/j.gca.2014.05.034, 2014.

Hatje, V., Masqué, P., Patire, V.F., Dórea, A., and Barros, F.: Blue carbon stocks, accumulation rates, and associated spatial variability in Brazilian mangroves, Limnol. Oceanogr., 9999: 1–14, doi: 10.1002/lno.11607, 2020.

680

Howard, J., Sutton-Grier, A., Herr, D., Kleypas, J., Landis, E., Mcleod, E., Pidgeon, E., and Simpson, S.: Clarifying the role of coastal and marine systems in climate mitigation, Front. Ecol. Environ., 15(1): 42-50, doi: 10.1002/fee.1451, 2017.

685

Jennarjahn, T.C.: Relevance and magnitude of 'Blue Carbon' storage in mangrove sediments: Carbon accumulation rates vs. stocks, sources vs. sinks, Estuar. Coast. Shelf S., 247, 107027, doi:10.1016/j.ecss.2020.107027, 2020.

[Jiménez Arias, J.L., Morris, E., Rubio de Inglés, M.J., Peralta, G., García Robledo, E., Corzo, A., and Papaspyrou, S.: Tidal elevation is the key factor modulating burial rates and composition of organic matter in a coastal wetland with multiple habitats, Sci. Total Environ., 724: 138205, doi:10.1016/j.scitotenv.2020.138205, 2020.](#)

690

Kauffman, J., Arifanti, V.B., Hernandez Trejo, H., del Carmen Jesús García, M., Norfolk, J., Cifuentes, M., Hadriyanto, D. and Murdiyarto, D.: The jumbo carbon footprint of a shrimp: carbon losses from mangrove deforestation, Front. Ecol. Environ., 15(4): 183-188, doi: /10.1002/fee.1482, 2017.

695

Kelleway, J.J., N. Saintilan, P.I. Macreadie, C.G. Skilbeck, A. Zawadzki, and P.J. Ralph.: Seventy years of continuous encroachment substantially increases 'blue carbon' capacity as mangroves replace intertidal salt marshes, Glob. Change Biol., 22 (3): 1097–1109, doi: 10.1111/gcb.13158, 2016.

Keil, R. G., and Mayer, L.M.: Mineral matrices and organic matter, in: Treatise on Geochemistry: Organic Geochemistry 2nd Edition Volume 12, edited by: Falkowski , P.G., Freeman, K.H., Holland, H. and Turekian, K., Elsevier, Amsterdam, Netherlands, doi:10.1016/B978-0-08-095975-7.01024-X, 337-359, 2014.

695 Komada, T., Reimers, C.E., Luther III, G.W., and Burdige, D.J.: Factors affecting dissolved organic matter dynamics
in mixed-redox to anoxic coastal sediments, *Geochim. Cosmochim. Ac.*, 68(20): 4099-4111, 2004.

Kristensen, E.: Mangrove crabs as ecosystem engineers; with emphasis on sediment processes, *J. Sea Res.*, 59, 30–
43, doi: 10.1016/j.seares.2007.05.004, 2008.

Kusumaningtyas, M.A., Hutahaeanc, A.A., Fischerd, H.W., Pérez-Mayod, M., Ransby, D., and Jennerjahn, T.C.:
700 Variability in the organic carbon stocks, sources, and accumulation rates of Indonesian mangrove ecosystems,
Estuar. Coast. Shelf S., 218, 310-323, doi: 10.1016/j.ecss.2018.12.007, 2019.

Lambs, L., Muller, E., and Fromard, F.: Mangrove trees growing in a very saline condition but not using seawater,
Rapid Commun. Mass Spectrom., 22: 2835–2843, doi: 10.1007/s10021-010-9329-2, 2008.

Lovelock, C.E., Sorrell, B.K., Hancock, N., Hua, Q., and Swales, A.: Mangrove forest and soil development on a
705 rapidly accreting shore in New Zealand, *Ecosystems*, 13(3): 437-451, doi: 10.1007/s10021-010-9329-2, 2010.

Lunstrum, A., and Chen, L.: Soil carbon stocks and accumulation in young mangrove forests, *Soil Biol. Biochem.*,
75, 223-232, doi: 10.1016/j.soilbio.2014.04.008, 2014.

MacKenzie, R.A., Foulk, P.B., Klump, J.V., Weckerly, K., Purbospito, J., Murdiyarso, D., Donato, D.C. and Nam,
V.N.: Sedimentation and belowground carbon accumulation rates in mangrove forests that differ in diversity and
710 land use: a tale of two mangroves, *Wetl. Ecol. Manag.*, 24(2): 245-261, doi: 10.1007/s11273-016-9481-3, 2016.

Marchand, C.: Soil carbon stocks and burial rates along a mangrove forest chronosequence (French Guiana), *Forest
Ecol. Manag.*, 384: 92-99, doi: 10.1016/S0272-7714(02)00134-8, 2017.

Marchand, C., Lallier-Vergès, E., and Baltzer, F.: The composition of sedimentary organic matter in relation to the
dynamic features of a mangrove-fringed coast in French Guiana, *Estuar. Coast. Shelf S.*, 56: 119–130, doi:
715 10.1016/S0272-7714(02)00134-8, 2003.

Marchand, C., Albe'ric, P., Lallier-Verge's, E., and Baltzer, F.: Distribution and characteristics of dissolved organic
matter in mangrove sediment pore waters along the coastline of French Guiana, *Biogeochemistry*, 81:59–75,
doi:10.1007/s10533-006-9030-x, 2006.

Matsumoto, K., Takanezawa, T., and Ooe, M.: Ocean tide models developed by assimilating TOPEX/POSEIDON
720 Altimeter Data into hydrodynamical model: a global model and a regional model around Japan, *J. Oceanogr.*,
56: 567–581, 200.

Matos, C.R., Berrêdo, J.F., Machado, W., Sanders, C.J., Metzger, E., and Cohen, M.C.: Carbon and nutrient
accumulation in tropical mangrove creeks, Amazon region, *Mar. Geo.*, 429: 106317,
doi:10.1016/j.margeo.2020.106317, 2020.

725 Mayer, L.M.: Relationships between mineral surfaces and organic carbon concentrations in soils and sediments,
Chem. Geol., 114: 347–363, doi:10.1002/lno.10478, 1994.

Miyajima, T., Hori, M., Hamaguchi, M., Shimabukuro, H., and Yoshida, G.: Geophysical constraints for organic carbon sequestration capacity of *Zostera marina* seagrass meadows and surrounding habitats, *Limnol. Oceanogr.*, 62(3): 954-972, doi:10.1002/lno.10478, 2017.

730 Miyajima, T., Y. Tsuboi, Y. Tanaka, and I. Koike.: Export of inorganic carbon from two Southeast Asian mangrove forests to adjacent estuaries as estimated by the stable isotope composition of dissolved inorganic carbon, *J. Geophys. Res.*, 114: G01024, doi:10.1029/2008JG000861, 2009.

Nellemann, C., Corcoran, E., Duarte, C.M., Valdés, L., De Young, C., Fonseca L, and Grimsditch, G.: Blue carbon: a rapid response assessment. United Nations Environment Programme, GRID-Arendal, 2009.

735 Nam, V.N., Sasmito, S.D., Murdiyarno, D., Purbopuspito, J., and MacKenzie, R.A.: Carbon stocks in artificially and naturally regenerated mangrove ecosystems in the Mekong Delta, *Wetl. Ecol. Manag.*, 24:231–244, doi: 10.1007/s11273-015-9479-2, 2016.

Nilsson, C. and Wilson, S.D.: Convergence in plant community structure along a disparate gradient: are lakeshores inverted mountainsides?, *The American Naturalist*, 137: 774-790, doi: 10.1086/285193, 1991.

740 Nordhaus, I., Salewski, T., and Jennerjahn, T.C.: Interspecific variations in mangrove leaf litter decomposition are related to labile nitrogenous compounds, *Estuar. Coast. Shelf. S.*, 192:137-148, doi:10.1016/j.ecss.2017.04.029, 2017.

Noguchi, K., Poungparn, S., Umnouysin, S., Patanaponpaiboon, P., Duangnamol, D., Yoneda, R., Utsugi, H., Sato, T., and Tabuchi, R.: Biomass and Production Rates of Fine Roots in Two Mangrove Stands in Southern Thailand, *JARQ*. 54(4): 349-360, doi:10.6090/jarq.54.349, 2020.

745 Parnell, A.C., Inger, R., Bearhop, S. and Jackson, A.L.: Source partitioning using stable isotopes: coping with too much variation, *PLoS one*, 5(3): e9672, doi:10.1371/journal.pone.0009672, 2010.

Pe'rez, A., Libardoni, B.G., Sanders, C.J.: Factors influencing organic carbon accumulation in mangrove ecosystems, *Biol. Letters*, 14: 20180237, doi:10.1098/rsbl.2018.0237, 2018.

750 Pickett, S.T.A.: Space-for-time substitution as an alternative to long-term studies, in: *Long-term studies in ecology*, edited by: Likens G. E., Springer, 110-135, 1989.

Primavera, J.H., Sadaba, R.S., Lebata, M.J.H.L., and Altamirano, J.R.: *Handbook of Mangroves in the Philippines – Panay*, SEAFDEC Aquaculture Department, Iloilo, Philippines, 106, 2004.

755 Salmo, S.G., Lovelock, C., and Duke, N.C.: Vegetation and soil characteristics as indicators of restoration trajectories in restored mangroves, *Hydrobiologia*, 720: 1–18, doi:10.1007/s10750-013-1617-3, 2013.

Prahl, F.G., Bennett, J.T., and Carpenter, R.: The early diagenesis of aliphatic hydrocarbons and organic matter in sedimentary particulates from Dabob Bay, Washington, *Geochimic. Cosmochim. Ac.*, 44, 1967–1976, 1980.

Prasad, M.B.K., Kumar, A., Ramanathan, A.L., and Datta, D.K.: Sources and dynamics of sedimentary organic matter in Sundarban mangrove estuary from Indo-Gangetic delta, *Ecological Processes*, 6:8, doi:10.1186/s13717-017-0076-6, 2017.

Pendleton, L., Donato, D.C., Murray, B.C., Crooks, S., Jenkins, W.A., Sifleet, S., Craft, C., Fourqurean, J.W., Kauffman, J.B., Marbà, N., and Megonigal, P.: Estimating global “blue carbon” emissions from conversion and degradation of vegetated coastal ecosystems, *PLoS One*, 7(9): e43542, doi: 10.1371/journal.pone.0043542, 2012.

Ranjan, R.K., Routh, J., Ramanathan, A.L., and Klump, J.V.: Elemental and stable isotope records of organic matter input and its fate in the Pichavaram mangrove-estuarine sediments (Tamil Nadu, India, Mar. Chem., 126, 163–172, doi: 10.1016/j.marchem.2011.05.005, 2011.

[Rasse, D.P., Rumpel, C., Dignac, M.-F. Is soil carbon mostly root carbon? Mechanisms for a specific stabilisation. Plant](#), 269, 341–356, 2005

Formatted: Font: (Default) Times New Roman, 10 pt

Ray, R., Michaud, E., Aller, R.C., Vantrepotte, V., Gleixner, G., Walcker, R., Devesa, J., Le Goff, M., Morvan, S. and Thouzeau, G.: The sources and distribution of carbon (DOC, POC, DIC) in a mangrove dominated estuary (French Guiana, South America), *Biogeochemistry*, 138(3), 297–321. doi:10.1007/s10533-018-0447-9, 2018.

Ray, R., Thouzeau, G., Walcker, R., Vantrepotte, V., Morvan, S., Devesa, J., Le Goff, M., and Michaud, E.: Mangrove-derived organic and inorganic carbon export to the Atlantic Ocean? Time series study in the Guianese estuarine system, Latin America, *J. Geophys. Res. Biogeosci.*, 125: 8, e2020JG005739, doi: 10.1029/2020JG005739, 2020.

Ren, H., Chen, H., Li, Z., and Han, W.: Biomass accumulation and carbon storage of four different aged Sonneratia apetala plantations in Southern China, *Plant. Soil*, 327: 279–291, doi: 10.1007/s11104-009-0053-7, 2010.

Shahraki, M., Fry, B., Krumme, U., and Rixen, T.: Microphytobenthos sustain fish food webs in intertidal arid habitats: a comparison between mangrove-lined and un-vegetated creeks in the Persian Gulf, *Estuar. Coast. Shelf Sci.*, 149: 203–212, doi: 10.1016/j.ecss.2014.08.017, 2014.

Shen, H., Tu, Z., You, G., Shi, X.: Grain Size and Pollen of Sediments in Wanghu Lake (Central China) Linked to Hydro-Environmental Changes, *Water*, 12, 45; doi:10.3390/w12010045, 2020.

Sasmito, S.D., Kuzyakov, Y., and Lubis, A.A.: Organic carbon burial and sources in soils of coastal mudflat and mangrove ecosystems, *Catena*, 187: 104414, doi: 10.1016/j.catena.2019.104414, 2020.

Sanders, C.J., Smoak, J.M., Naidu, A.S., Sanders, L.M., and Patchineelam, S.R.: Organic carbon burial in a mangrove forest, margin and intertidal mud flat, *Estuar. Coast. Shelf S.*, 90: 168–172, doi: 10.1016/j.ecss.2010.08.013, 2010.

Sharma, S., MacKenzie, R.A., Tieng, T., Soben, K., Tulyasuwon, N., Resanond, A., Blate, G. and Litton, C.M.: The impacts of degradation, deforestation and restoration on mangrove ecosystem carbon stocks across Cambodia, *Sci. Total Environ.*, 706, 135416, doi: 10.1016/j.scitotenv.2019.135416. 2020.

790 Sheehan, L., Sherwood, E., Moyer, R.P., Radabaugh, K.R., and Simposon, S.: Blue carbon: an additional driver for restoring and preserving ecological services of coastal wetlands in Tampa Bay (Florida, USA), *Wetlands*, 39: 1317–1328, doi: 10.1007/s13157-019-01137-y, 2019.

795 Smith III, T. J., Boto, K. G., Frusher, S. D., and Giddins, R. L.: Keystone species and mangrove forest dynamics: the influence of burrowing by crabs on soil nutrient status and forest productivity, *Estuar. Coast. Shelf. S.*, 33: 419–432, doi:10.1016/0272-7714(91)90081-L, 1991.

Soper, F.M., MacKenzie, R.A., Sharma, S., Cole, T.G., Litton, C.M., and Sparks, J.P.: Non - native mangroves support carbon storage, sediment carbon burial, and accretion of coastal ecosystems, *Glob. Change Biol.*, 25:4315–4326, doi: 10.1111/gcb.14813, 2019.

800 [Tue, N.T., Dung, L.V., Nhuan, M.T., Omori, K.: Carbon storage of a tropical mangrove forest in Mui Ca Mau National Park, Vietnam. Catena, 121, 119–126, 2011.](#)

Formatted: Font: (Default) Times New Roman, 10 pt

Formatted: Font: (Default) Times New Roman, 10 pt

Formatted: Font: (Default) Times New Roman, 10 pt

Formatted: Font: 9 pt

Van Hieu, P., Dung, L.V., Tai Tue, N., and Omori, K.: Will restored mangrove forests enhance sediment organic carbon and ecosystem carbon storage?, *Regional Studies in Marine Science*, 14: 43–52, doi: 10.1016/j.rsma.2017.05.003, doi: 10.1016/j.rsma.2017.05.003, 2017.

805 Valiela, I., Bowen, J. L. and York, J. K.: Mangrove forests: one of the world's threatened major tropical environments, *Bioscience*, 51:807–815, doi: 10.1641/0006-3568(2001)051[0807:MFOOTW]2.0.CO;2, 2001.

Wagai, R., Mayer, L.M., and Kitayama, K.: Extent and nature of organic coverage of soil mineral surfaces assessed by a gas sorption approach, *Geoderma*, 149: 152-160, doi: 10.1016/j.geoderma.2008.11.032, 2009.

810 Wang, G., Yu, C., Singh, M., Guan, D., Xiong, Y., Zheng, R. and Xiao, R.: Community structure and ecosystem carbon stock dynamics along a chronosequence of mangrove plantations in China, *Plant Soil*, 464: 605–620, doi: 10.1007/s11104-021-04973-2, 2021.

Walker, L. R., Wardle, D. A., Bardgett, R. D., and Clarkson, B. D.: The use of chronosequences in studies of ecological succession and soil development, *J. Ecol.*, 98, 725–736, doi:10.1111/j.1365-2745.2010.01664.x, 2010.

815 Walcker, R., Gandois, L., Proisy, C., Corenblit, D., Mougin, É., Ray, R., and Fromard, F.: Control of 'blue carbon' storage by mangrove ageing: evidence from a 66-year-chronosequence in French Guiana, *Glob. Change Biol.*, 24: 2325-2338, doi: doi.org/10.1111/gcb.14100, 2018.

Formatted: Font: (Default) Times New Roman, 10 pt

Formatted: Font: (Default) Times New Roman, 10 pt

Formatted: Font: (Default) Times New Roman, 10 pt, Not Italic

Formatted: Font: Not Italic

Formatted: Font: (Default) Times New Roman, 10 pt, Not Bold

Formatted: Font: (Default) Times New Roman, 10 pt

[Xia M, Talhelm AF, Pregitzer KS.: Fine roots are the dominant source of recalcitrant plant litter in sugar maple-dominated northern hardwood forests. New Phytol. 208; 715– 726, 2015.](#)

820 Xiong, Y., Liao, B., and Wang, F.: Mangrove vegetation enhances soil carbon storage primarily through in situ inputs rather than increasing allochthonous sediments, *Mar. Pollut. Bull.*, 131: 378-385, doi:10.1016/j.marpolbul.2018.04.043, 2018.

Yoshikai, M., Nakamura, T., Suwa, R., Argamosa, R., Okamoto, T., Rollon, R., Basina, R., Primavera-Tirol, Y.H., Blanco, A.C., Adi, N.S. and Nadaoka, K.: Scaling relations and substrate conditions controlling the complexity of Rhizophora prop root system, *Estuar. Coast Shelf S.*, 248:107014, doi:10.1016/j.ecss.2020.107014, 2021.

Zhang, Y., Xiao, L., Guan, D., Chen, Y., Motelica-Heino, M., Peng, Y. and Lee, S.Y.: The role of mangrove fine root production and decomposition on soil organic carbon component ratios, *Ecol. Indic.*, 125: 107525, doi:10.1016/j.ecolind.2021.107525, 2021.

Figure legends

Figure 1: Map of the study area. BS (Bare sediment); PM (Pioneer mangrove, 3-month); YM (Young mangrove, 10-yr); AM (Adult mangrove, 20-yr); MM (Mature mangrove, 30-yr). The circle shows presence of long-tailed sandbar between AM and YM site. The north-west inland part and bank of the Aklan River are the dominant places for the naturally occurring mangroves.

Formatted: Font: 10 pt

Figure 2: Variation of physical and biogeochemical parameters (mean±SD) in the sediments according to mangrove development. **nd: no data available**

Formatted: Font: 10 pt

Figure 3: Vertical profiles of sedimentary carbon properties during wet and dry season.

Figure 4: Vertical distribution of sediment surface area and OC loading during wet and dry season

Figure 5: Vertical profiles of porewater DOC during wet and dry season

Figure 6: Source identification of sedimentary organic matter using endmember carbon stable isotope ratio and OC:TN.

Figure 7: Source apportionment of sedimentary organic matter at different mangrove stages by applying bayesian mixing model with $\delta^{13}\text{C}$ and OC:TN.

Figure 7a: a) The relationship between mangrove age (Age) and carbon stock (OC), where the curve was drawn based on an exponential function model in Eq. 2: $OC = 171.07\exp(0.03558*Age)$, $R^2 = 0.9873$. The gray band means 95% confidence interval. (b) The relationship between mangrove age and carbon accumulation rate (CAR) on the basis of the exponential model (see Eq. 3).

Slopes derived from linear and exponential relationship between (a) mangrove age and carbon stock (b) and carbon accumulation rate (CAR).

Formatted: Font: (Default) Times New Roman, 10 pt

Formatted: Font: (Default) Times New Roman, 10 pt, Bold

Formatted: Normal, Indent: Left: 0", Hanging: 0.5", Line spacing: 1.5 lines

Formatted: Font: 10 pt

Table 1: The significance of effects of season, type and depth to TOC, DOC, bulk OC/TN ratio $\delta^{13}\text{C}$ and $\delta^{15}\text{N}$ using ANOVA
 855 on the basis of the generalized additive model (GAM). In the parameter of depth, the approximate significance
 of smooth term is shown.

| Parameters | Season | Type | Depth |
|-----------------------|---------------|--------------|--------------|
| TOC | 0.0855 | ≤ 0.001 | ≤ 0.001 |
| DOC | 0.1986 | 0.003 | 0.127 |
| OC:TN | ≤ 0.001 | ≤ 0.001 | 0.033 |
| $\delta^{13}\text{C}$ | 0.0656 | ≤ 0.001 | 0.411 |
| $\delta^{15}\text{N}$ | 0.0148 | 0.0061 | 0.737 |

860 Formatted Table

| Parameters | Season | Type | Depth |
|-----------------------|---------------|--------------|--------------|
| TOC | 0.0855 | ≤ 0.001 | ≤ 0.001 |
| DOC | 0.1986 | 0.003 | 0.127 |
| OC:TN | ≤ 0.001 | ≤ 0.001 | 0.033 |
| $\delta^{13}\text{C}$ | 0.0656 | ≤ 0.001 | 0.411 |
| $\delta^{15}\text{N}$ | 0.0148 | 0.0061 | 0.737 |

865

870

875

880

885

890 **Table 2. Contribution (%) of endmember sources to sediment organic matter. POM: Particulate
 Organic Matter, MPB: Microphytobenthos AM: adult mangrove, MM: mature mangrove, PM:
 pioneer mangrove, YM: young mangrove. Bare sediment or BS was set as reference level.
 Mean±SD (mean at 95% confidence level)**

895

| Sampling site | Mangrove leaf (%) | Marine POM (%) | MPB (%) | River POM (%) |
|---------------|-------------------|----------------|----------|---------------|
| BS | 18±14 (45) | 18±21 (67) | 6±9 (25) | 58±28 (92) |
| PM | 32±17 (63) | 18±19 (59) | 7±9 (29) | 43±24 (83) |
| YM | 53±16 (77) | 13±11 (40) | 5±6 (18) | 29±18 (60) |
| AM | 41±14 (64) | 14±12 (40) | 5±4 (16) | 39±18 (68) |
| MM | 58±19 (86) | 11±9 (31) | 5±4 (13) | 29±19 (66) |

900

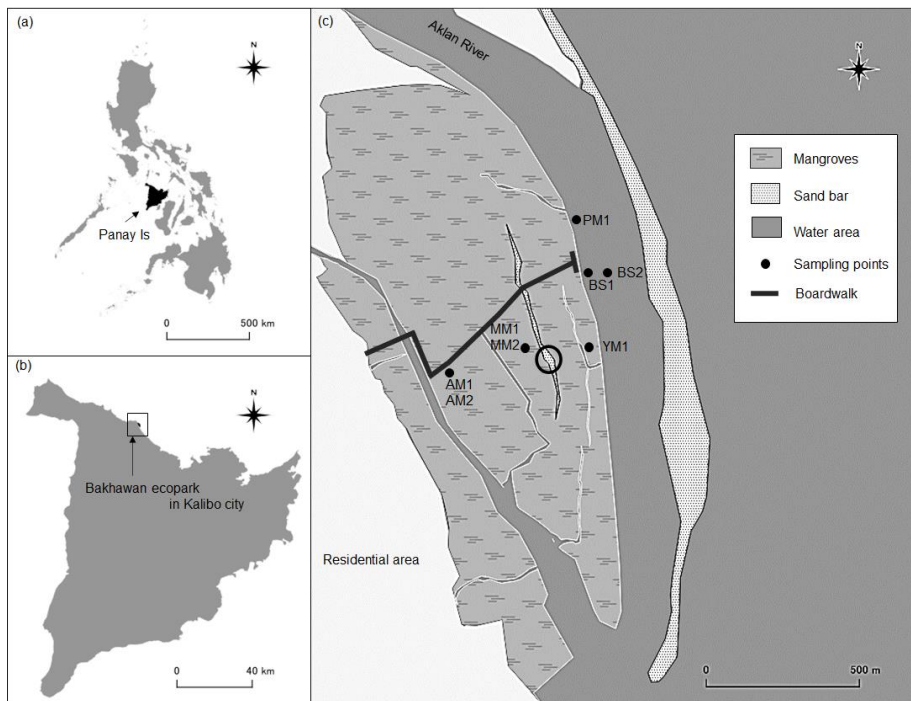
905

910

915

Table 3. Comparative results on carbon stock (Mg C ha⁻¹) in restored mangroves of known ages, and organic carbon loading (μmol C m⁻²) in mangrove with other marine settings.

| Location | Age (year) | Dominant species | Soil C stock Mg C ha ⁻¹ | OC loading μmol C m ⁻² | Reference |
|---------------------------|------------|--|------------------------------------|-----------------------------------|-----------------------------------|
| Philippines, Panay | | | | | |
| Bakhanwan EP | 0 | No vegetation | 3.1-24.3 | 4-58 | This study |
| Bare sediment | | | | | |
| Pioneer | 0.25 | <i>Avicennia marina</i> , <i>Rhizophora spp</i> | 21.4 | ± | This study |
| Young | 10 | <i>Rhizophora apiculata</i> | 23.1 | ± | This study |
| Adult | 20 | <i>Rhizophora apiculata</i> | 36.9-46.4 | 42-148 | This study |
| Mature | 30 | <i>Rhizophora apiculata</i> | 61.3-93.5 | 68-380 | This study |
| Planted | ± | <i>Rhizophora sp.</i> | ± | 310-1140 | Unpublished data, Miyajima et al. |
| Naturally recovered | ± | <i>Avicennia Rumphiana</i> | ± | 57-640 | Unpublished data, Miyajima et al. |
| North-central Vietnam | 0 - 27 | <i>Kandelia obovata</i> | 54 - 84 | ± | Van Hieu et al., 2017 |
| Pichavaram, India | 12-21 | <i>Rhizophora spp</i> | 41-94 | ± | Gnanamoorthy et al., 2019 |
| Bhitarkanika, India | 5 | <i>Kandelia candel</i> | 38 | ± | Bhomia et al., 2016 |
| Sulawesi, Indonesia | >10 | <i>Rhizophora apiculata</i> | 150-300 | ± | Cameron et al., 2019 |
| Continental margin | ± | ± | ± | 40-80 | Mayer, 1994 |
| Vegetated marine sediment | ± | ± | ± | 56-67 | Miyajima and Hamaguchi, 2017 |
| Floodplain | ± | ± | ± | 16-42 | Goni et al., 2014 |

**Fig. 1.**

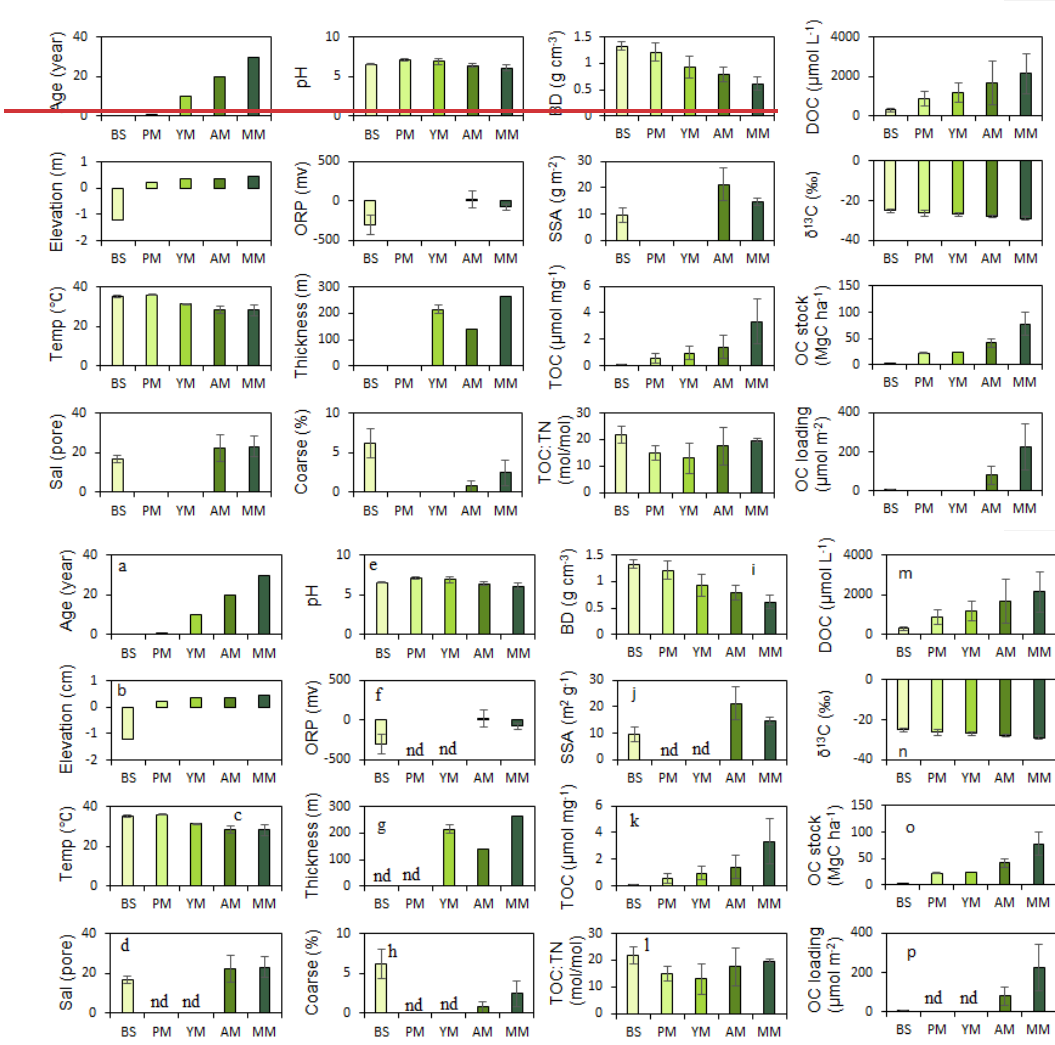


Fig. 2.

950

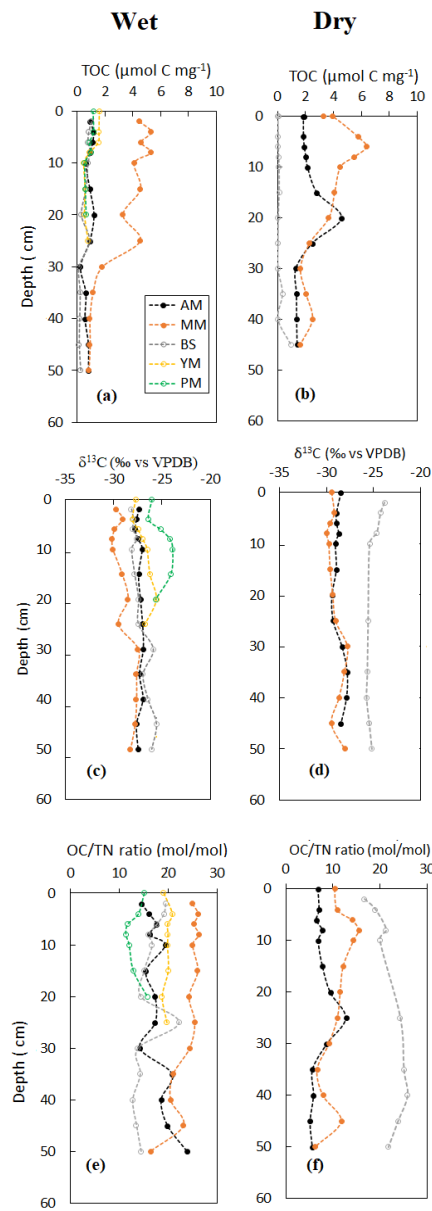
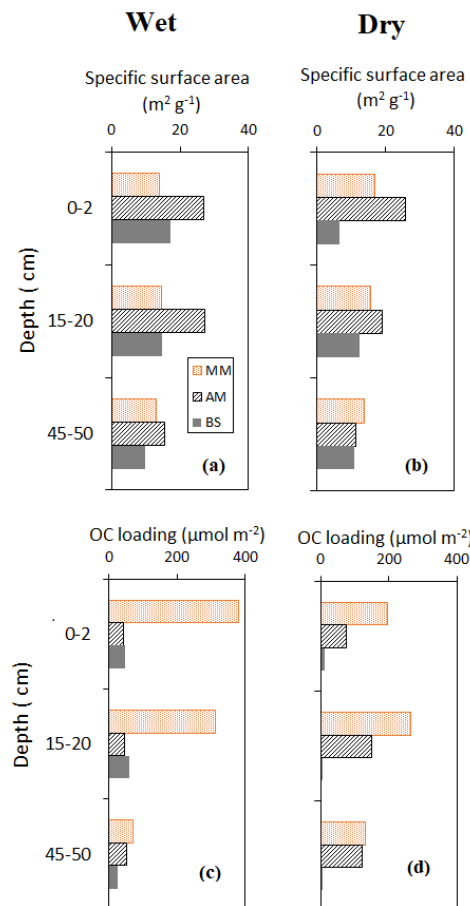
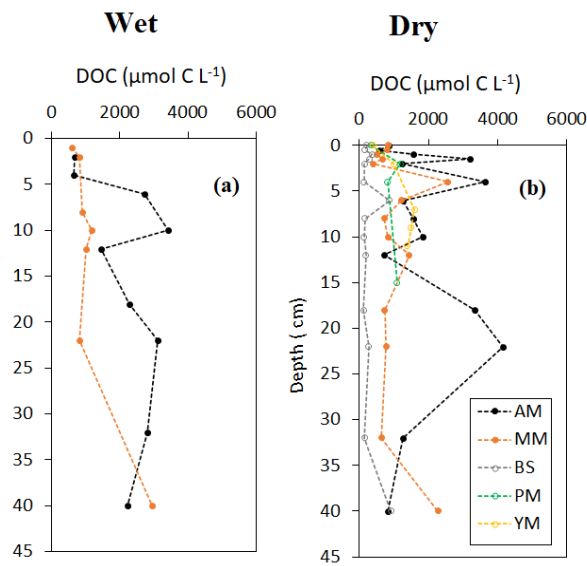


Fig. 3.



955 **Fig. 4.**

960

**Fig. 5.**

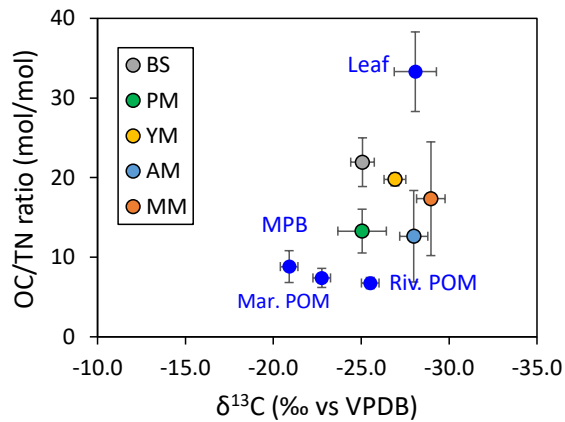


Fig. 6.

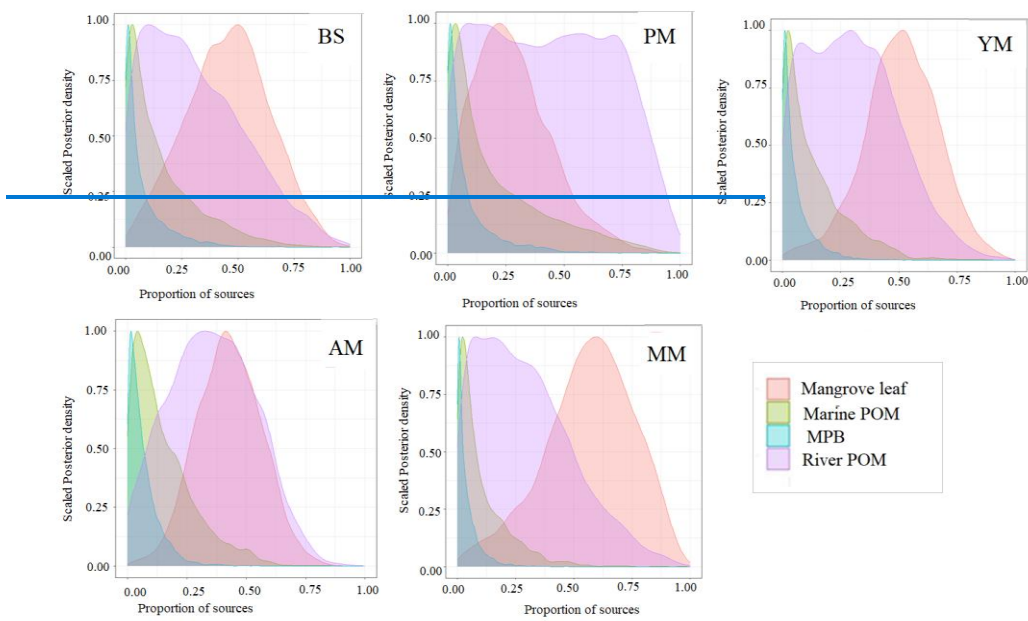
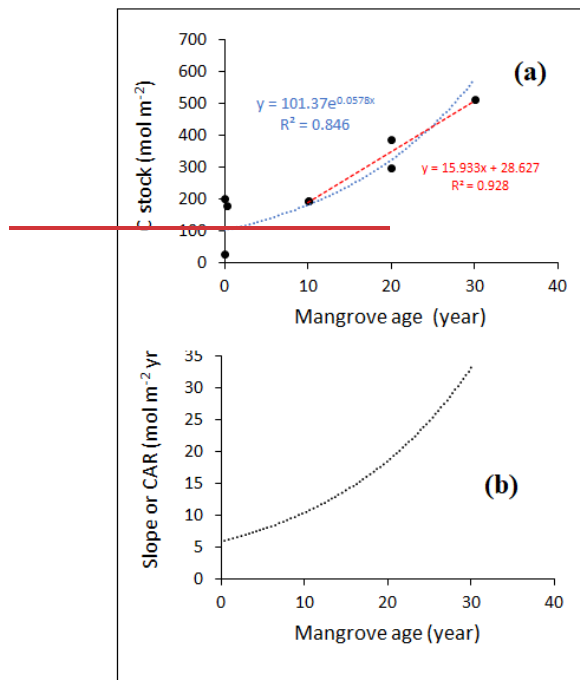


Fig. 67.



985

990

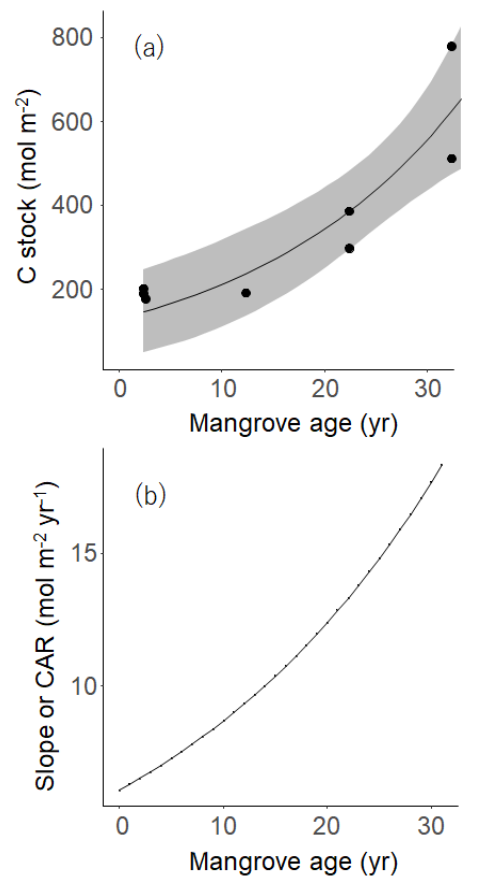


Fig. 78.

995

1000

1005

1010